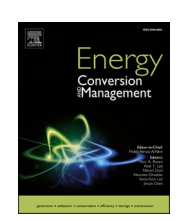
ELSEVIER

Contents lists available at ScienceDirect

Energy Conversion and Management

journal homepage: www.elsevier.com/locate/enconman





Flexible CO₂-plume geothermal (CPG-F): Using geologically stored CO₂ to provide dispatchable power and energy storage

Mark R. Fleming ^a, Benjamin M. Adams ^b, Jonathan D. Ogland-Hand ^b, Jeffrey M. Bielicki ^{c,d}, Thomas H. Kuehn ^a, Martin O. Saar ^{b,e,*}

- a Department of Mechanical Engineering, University of Minnesota, 111 Church St SE, Minneapolis, MN 55455, USA
- ^b Geothermal Energy and Geofluids Group, Department of Earth Sciences, ETH Zurich, Sonneggstrasse 5, 8092 Zurich, Switzerland
- Department of Civil, Environmental, and Geodetic Engineering, 2070 Neil Avenue, Columbus, OH 43210, USA
- ^d John Glenn College of Public Affairs, 1810 College Road, Columbus, OH 43210, USA
- ^e Department of Earth and Environmental Sciences, University of Minnesota, 116 Church Street SE, Minneapolis, MN 55455, USA

ARTICLE INFO

Keywords: Carbon Dioxide Geothermal Energy Renewable Energy Carbon Dioxide Plume Geothermal (CPG) Large-scale energy storage Operational Strategies

ABSTRACT

 CO_2 -Plume Geothermal (CPG) power plants can use geologically stored CO_2 to generate electricity. In this study, a Flexible CO_2 Plume Geothermal (CPG-F) facility is introduced, which can use geologically stored CO_2 to provide dispatchable power, energy storage, or both dispatchable power and energy storage simultaneously—providing baseload power with dispatchable storage for demand response. It is found that a CPG-F facility can deliver more power than a CPG power plant, but with less daily energy production. For example, the CPG-F facility produces 7.2 MWe for 8 h (8 h-16 h duty cycle), which is 190% greater than power supplied from a CPG power plant, but the daily energy decreased by 61% from 60 MWe-h to 23 MWe-h. A CPG-F facility, designed for varying durations of energy storage, has a 70% higher capital cost than a CPG power plant, but costs 4% to 27% more than most CPG-F facilities, designed for a specific duration, while producing 90% to 310% more power than a CPG power plant. A CPG-F facility, designed to switch from providing 100% dispatchable power to 100% energy storage, only costs 3% more than a CPG-F facility, designed only for energy storage.

1. Introduction

Least-cost pathways that limit the increase of global mean surface temperatures to 2 $^{\circ}$ C, or less, rely on decarbonizing the electricity sector by transitioning to a portfolio of low-carbon energy technologies and processes that work synergistically to meet electricity demand [1–5]. For example, future least-cost decarbonized electricity systems will likely be comprised of technologies and processes that provide 1) electricity generation from variable renewable resources (e.g., wind, sunlight), 2) balancing services (e.g., batteries, demand response) that adjust supply or demand, 3) carbon-dioxide (CO₂) storage services (e.g., as part of a CO₂ capture and storage (CCS) process) that permanently isolate emissions from the atmosphere by storing them in deep naturally porous and permeable aquifers, and 4) dispatchable power that can be delivered whenever needed (e.g., flexible nuclear power plants, fossilfuel power plants that are part of CCS processes) [6–8]. As a result of this synergistic operation, low-carbon electricity system technologies or

processes that can provide more than one of these four services will likely be valuable.

CO₂ was initially proposed as a working fluid in Enhanced Geothermal Systems (EGS) by Brown [9]. CO₂ has three primary advantages over brine: 1) in contrast to liquid water, CO₂ is highly compressible, allowing the system to generate a thermosiphon, reducing or eliminating the need for circulation pumps [9–13], 2) CO₂ has a lower kinematic viscosity which reduces the pressure losses through the rock in the reservoir [14,15], and 3) CO₂ has a lower mineral solubility that will reduce pipe and equipment scaling [9]. In CO₂-EGS systems, CO₂ was found to have higher heat extraction rates than brine and develop a thermosiphon [10,11,16]. However, CO₂-EGS has large-scale deployment issues, for example, it has a limited CO₂ storage potential due to the limited volume of the fractured reservoir [17,18]. In contrast, a different CO₂-based geothermal system, first introduced by Randolph and Saar [17], who termed it CO₂-Plume Geothermal (CPG), uses common and expansive sedimentary basins with low-permeability

Abbreviation: CPG, Carbon Dioxide Plume Geothermal.

* Corresponding author.

E-mail address: saarm@ethz.ch (M.O. Saar).

caprocks that limit the leakage of buoyant CO_2 [19–22]. These basins have large CO_2 storage potential and are a target for Carbon Capture and Storage (CCS) efforts [19,23]. Previous studies have shown the effectiveness of CPG systems at extracting heat and pressure energy from subsurface reservoirs [17,18,24–28], power production driven by a thermosiphon [29], the benefits of using CO_2 over brine in sedimentary basins [12,30,31], and how CPG can be used in depleted natural gas reservoirs [33] or depleted oil reservoirs [34].

Recent efforts have investigated technologies that use geologically stored CO2 from CCS processes and geothermal energy resources to provide energy storage or dispatchable power: CO2-Plume Geothermal (CPG) power plants [12,29,35,36], CO₂-Bulk Energy Storage (CO₂-BES) facilities [37], and Compressed CO2 Energy Storage (CCES) facilities [38]. For example, CPG power plants provide dispatchable power by intentionally producing geologically stored CO2 to the surface, expanding it through a turbine to generate electricity, then cooling, condensing, and re-injecting it into the subsurface [12,24,26,29,39]. CCES facilities use CO₂ compressed in a multi-level subsurface reservoir in combination with a surface heat source to provide energy storage. CO₂-BES facilities, in contrast, can provide dispatchable power or energy storage by alternating the timing of fluid (CO₂ and/or brine) injection, production, and re-injection [40]. As a result, these CO₂-geothermal energy systems are likely to have value to decarbonization efforts because they can directly reduce CO2 emissions by sequestering them in the subsurface while indirectly reducing CO2 emissions by working with other low-carbon technologies to meet demand [41].

This paper introduces another novel development in CO₂-geothermal energy systems: Flexible-CO2 Plume Geothermal (CPG-F) facilities. A CPG-F facility is distinguished from a standard CPG power plant because CPG-F facilities make use of a second, shallower aquifer within a given sedimentary basin geothermal resource, which enables additional operational capabilities compared to previously studied CPG power plants. In CPG-F facilities, geothermally-heated CO2 is produced to the surface as during standard CPG power plant operations, expanded through a high-pressure turbine to produce power, and then the option exists to either a) inject a portion or all of the expanded CO2 in the shallow reservoir for temporary storage or b) expand the CO2 through another low-pressure turbine to produce more power before cooling and reinjecting it into the deeper reservoir like in a standard CPG power plant. If CO2 is injected into the shallow reservoir, CPG-F operators would later produce it back to the surface, cool it, and then reinject it into the deeper reservoir. Temporarily storing the CO2 in the shallow reservoir effectively time-shifts the parasitic cooling and pumping power loads, thus allowing CPG-F facilities to provide energy storage services for demand response. In this way, CPG-F facilities are similar to CO2-BES facilities because they can provide energy storage or dispatchable power, but by only circulating CO2. In contrast to CO2-BES facilities, however, because it is possible to only divert a portion of the produced CO2 to shallow reservoir storage, a CPG-F facility can also provide both dispatchable power and energy storage, simultaneously-providing baseload power with dispatchable storage for demand response. A CPG-F system is different from other CO2-based subsurface energy storage systems. For example, a CO2-Bulk Energy Storage (CO₂-BES) system uses a reservoir that is initially filled with native brine, into which CO2 is injected and used as a cushion gas to moderate the reservoir pressure during disjoint brine production and injection phases [42,43]. The produced brine must be stored at the surface, and the differences between the brine production and injection phases provide the energy generation and storage, much like a pumped hydroelectric energy storage system. Compressed CO2 Energy Storage (CCES) is another approach. It is similar to a CPG-F system, in that it exchanges CO₂ between high- and low-pressure reservoirs [38], but the CCES system only uses geothermal heat to pre-heat the CO₂; most of the heat is added at the surface by combusting a fuel. Thus, CPG-F is a unique system that operates primarily with geologic CO2, requires no surface storage of fluid, and has no fossil fuel heat source.

Given the flexibility of this system, there are more questions to address when designing a CPG-F facility compared to designing a CPG power plant. For example, what service to provide? What $\rm CO_2$ production flowrate should the facility be designed around? If the CPG-F facility will not be providing strictly dispatchable power (i.e., a CPG power plant), over what duration(s) will the CPG-F facility time-shift electricity? These questions are not independent, and the answers will vary depending on the cost and performance of the CPG-F facility, the value of the provided service(s) to the electricity system, and the rate at which CPG-F operators are compensated by electric market rules for providing the service(s).

In this study, as a starting point towards answering these interdependent questions, we provide an initial investigation into the performance and capital cost of a CPG-F facility designed to provide different services. We focus primarily on CPG-F facilities designed to provide only energy storage because our prior work focuses on systems that provide only dispatchable power (i.e., CPG power plants) and it is unknown if providing both dispatchable power and energy storage services simultaneously has value to the electricity system. Section 2 provides an overview of the CPG-F system and the tools and methods used to simulate its operation and estimate cost; Section 3 compares a CPG power plant to a CPG-F facility by presenting optimal operational decisions (e.g., CO₂ production flowrates) across a range of diurnal energy storage duty cycles that a) maximize net energy production, b) maximize power production, c) zero-out the daily net energy storage, and d) minimize cost; and Section 4 discusses the primary findings and potential avenues for future work.

2. Methods

Section 2.1, presents a description of a CPG-F facility and how the components are operated to provide different services. Following that identification, Section 2.2 describes how CPG-F is modeled, and then

Table 1Nomenclature

Variable	Parameter
A C f g η h λ M m mf	Area [m²] Cost [\$] Friction factor [-] Gravitational acceleration [m/s²] Efficiency [-] Enthalpy [kJ/kg] Parasitic loss fraction [-] Daily CO ₂ Circulation Rate [kt/day] Mass Flow Rate [kg/s] Mass Fraction [-]
rry P Q	Pressure [kPa] Heat Rejection [kW]
ρ SCC T t TPCC V W	Density [kg/m³] Specific Capital Cost [\$/kWe] Temperature [°C] Time [h] Total Project Capital Cost [\$] Velocity [m/s] Power [kWe]
W x Z z	Energy [kW _e -h] Cost Fraction [-] Reservoir Thickness [m] Reservoir Depth [m] Description
MW _e MW _{th} MW _e -h MW _{th} -h Kt Mt	Megawatt (electrical) Megawatt (thermal) Megawatt hour (electrical) Megawatt hour (thermal) Kiloton (metric) Megaton (metric)

Section 2.3 provides the cost analysis methodology. The nomenclature is defined in Table 1.

2.1. Overview of CPG-F

This section presents a system diagram differentiating how a single CPG-F facility would be operated to provide three different services, if designed to do so: 1) dispatchable power, 2) energy storage, or 3) both dispatchable power and energy storage simultaneously.

2.1.1. CPG-F operated to provide dispatchable power

The solid red lines in Fig. 1 highlight the system components that are used when CPG-F is operated to provide dispatchable power: a deep porous and permeable aquifer beneath a low- to zero-permeability caprock, a surface power plant, and vertical injection and production wells [17,18,25]. Geologically stored CO2 that is heated by the geothermal heat flux (State 1) is produced from the geothermal reservoir to the surface through vertical wells (State 2). That CO₂ is expanded in a high-pressure turbine (HPT) (State 3) and a low-pressure turbine (LPT) (State 4) to generate electricity. These turbines are shown separately, but they may be combined into a single stage if the CPG-F facility is designed to only provide dispatchable power (i.e., a CPG power plant). After the turbines, the CO_2 is cooled using a wet cooling tower (State 5). If used, a production pump can increase the pressure of the CO₂ (State 6) to achieve the necessary downhole pressure (State 7). A production pump is not required to drive fluid production, but using one generally increases the net power production of the system [12,29].

2.1.2. CPG-F operated to provide energy storage

When a CPG-F facility is operated to provide energy storage, the shallow reservoir is used to temporally store the $\rm CO_2$, effectively creating two different processes from the surface components – one using the power cycle components that produce power (i.e. the turbine), and the other that uses the components that store, or consume, power (i.e. the cooling towers and the pump). Energy storage occurs by alternating between two modes:

Electricity Generation (Dispatch) (Green lines in Fig. 1): The CO₂ is produced from the deep reservoir (State 1), brought to the surface in the production well (State 2), and expanded in the HPT (State 3) to produce power. After the HPT, the CO₂ is minimally cooled in a cooling tower (State 8) to increase the density of the CO₂ enough to obtain the necessary downhole pressure to inject the CO₂ into the shallow reservoir (State 9). By increasing the CO₂ density in the

- injection well, the downhole pressure is increased, which is less energy intensive than pumping [44]. In the shallow reservoir, the $\rm CO_2$ is stored isothermally. During this mode, the gross turbine power less the parasitic power—the power required to operate the pre-injection cooling tower (States 2 to 8)—is positive.
- 2. **Power Consumption (Storage) (Blue lines in Fig. 1):** The CO₂ that is stored in the shallow reservoir (State 10) is produced to the surface through the vertical well (State 11). Then, similar to when the CPG-F facility is operated for dispatchable power, the density of the CO₂ is increased in the cooling towers (State 5), it is pumped (State 6), and reinjected into the deep reservoir (State 7). Although shown in Fig. 1, the throttling valve between States 11 and 4 is not used when a CPG-F facility is designed to only provide energy storage as a stand-alone system because the pressure in the cooling tower (State 4) is equivalent to the wellhead pressure from the shallow reservoir (State 11).

When operating to provide energy storage, the shallow reservoir is used to temporarily store CO_2 and is not the primary source of extracting geothermal heat. Also, note that when operated to provide energy storage, a CPG-F facility cannot use the LPT that is used when operated to provide dispatchable power. The same pressure difference between States 3 and 4 that is used for generating dispatchable power in the LPT is lost in piping and reservoir frictional losses when storing CO_2 in the shallow reservoir. Thus, the thermal efficiency of CPG-F facility when operating to provide energy storage will be inherently lower than when operating to provide dispatchable power.

2.1.3. CPG-F operated to provide both dispatchable power and energy storage simultaneously

The facility operates continuously to generate dispatchable electricity, while also providing either additional power production (electricity generation mode) or power consumption (storage mode). Despite being called the storage mode, the combined power output of the CPG-F facility operated in this way may still be positive if the power that is being consumed is less than the dispatchable power that being produced at the same time.

When a CPG-F facility is operated to provide dispatchable power and to produce power that was previously stored, the CO_2 stream is split after the high-pressure turbine (State 3). The fraction of CO_2 for energy storage is cooled (State 8) and injected into the shallow reservoir for storage (State 9). The remaining CO_2 stream is further expanded in the low-pressure turbine (State 4) to produce power, then cooled (State 5), compressed (State 6), and re-injected back into the deep reservoir (State 7). The split flow stream allows the system to vary from operating 100%

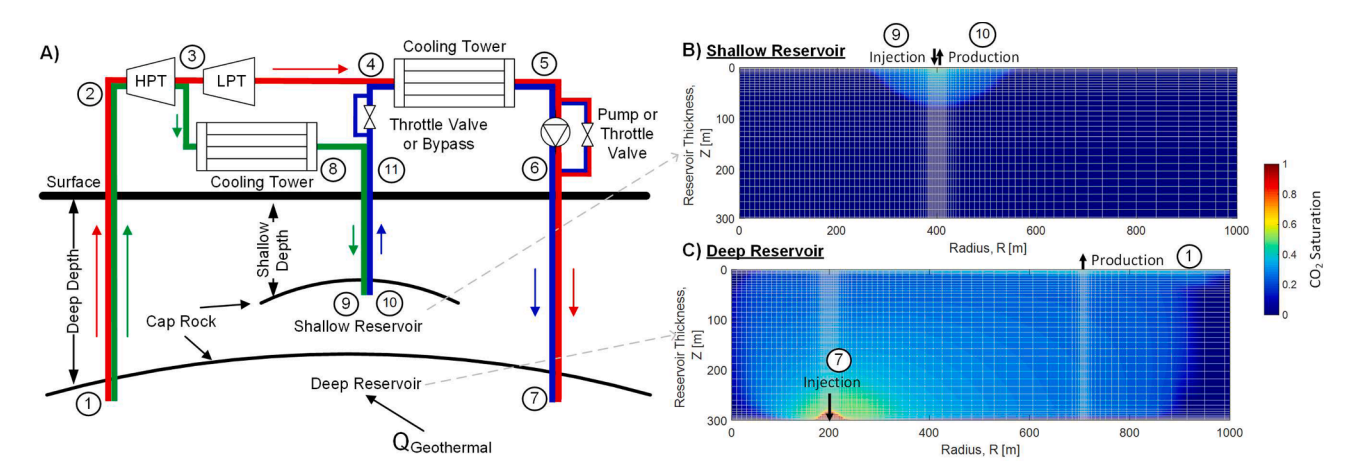


Fig. 1. (A) System diagram for a CPG-F facility operating to provide dispatchable power (red lines), energy storage (blue lines for power consumption; green lines for power generation), and both services simultaneously (red + green + blue lines). The CO_2 gas saturation with mesh grid overlay of the shallow (B) and deep (C) reservoirs at the end of the CO_2 plume development period and start of the energy storage operation. (For interpretation of the references to colour in this figure legend, the reader is referred to the web version of this article.)

for dispatchable power to operating 100% for energy storage, designated by the mass flow rate division, detailed in Section 2.2.2.

When the CPG-F facility is operated to provide dispatchable power and to consume (store) additional power for later, the fraction of CO_2 for energy storage is produced from the shallow reservoir (State 10), arrives at the surface (State 11), is throttled to the turbine back-pressure (State 4), and then re-combined with the CO_2 stream leaving the low-pressure turbine. The produced CO_2 is typically supercritical at the wellhead pressure (State 11) and thus larger than the LPT backpressure (State 4). Additionally, the wellhead pressure decreases as the shallow reservoir depletes of CO_2 . Thus, a throttling valve is added to reduce the wellhead pressure (State 11) to the constant condenser pressure (State 4).

2.2. System modeling

The CPG-F facilities are simulated using two separate models: the subsurface reservoir model and the surface power plant model. The subsurface reservoir is modeled using TOUGH2 [45] with the ECO2N [46] equation of state module. The wells and the surface power plant are modeled using Engineering Equation Solver (EES) [47]. The computational workflow constitutes: 1) simulate the deep reservoir, 2) simulate the shallow reservoir, 3) input the reservoir model output into the well and surface power plant model; then these steps are iterated for each mass flow rate and duty cycle.

2.2.1. Reservoir modeling

An overview of the multi-reservoir system with the injection and production well design is shown in Fig. 2. Each reservoir is a two-dimensional, axisymmetric model using the reservoir parameters given in Table 2. The reservoirs are initially filled with 20% NaCl (by weight) brine. Both the deep and the shallow reservoirs have horizontal and

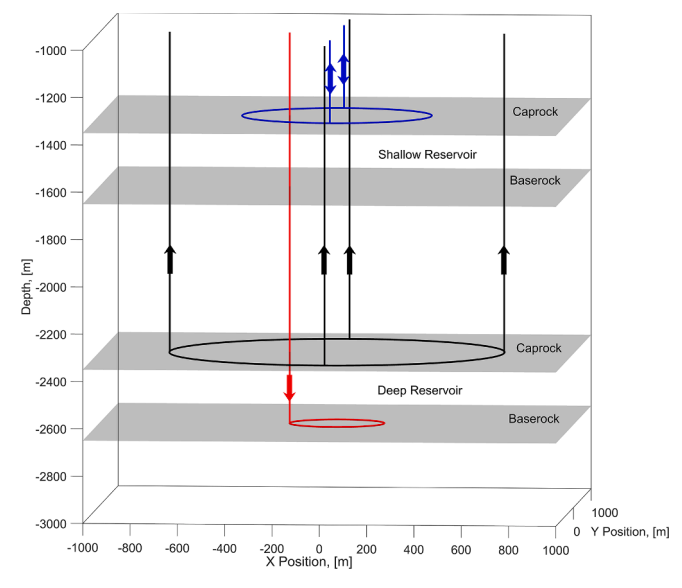


Fig. 2. An overview of the horizontal and vertical well configuration for both the shallow reservoir (blue wells) and the deep injection (red wells) and the deep production wells (black). The bounding caprock and baserock formations are indicated in the figure by the gray planes. The shallow well (blue) is a huff-and-puff well as minimal heat exchange with the surrounding formation is desired. The deep reservoir is accessed via a deeper injection well (red) and fluid (mostly CO₂) is produced from production wells (black), where the horizontal collection well component is located immediately below the caprock (see also Fig. 1). Note that in practice, the horizontal wells would likely not be circular but rather linear or bent as the CO₂ plume is likely to be diverted in a preferred direction (up-caprock-dip) as described in Garapati et al. (2015) [24]. Circular wells are chosen here mainly as they simplify numerical modeling and figure display. (For interpretation of the references to colour in this figure legend, the reader is referred to the web version of this article.)

 Table 2

 Reservoir physical properties for the numerical simulation.

Simulated Parameter/Value				
General Properties		Deep Reservoir		
Horizontal	$5.0 \times 10^{-14} \text{ m}^2 \text{ (50)}$	Mean Reservoir	2.5 km	
Permeability	mD)	Depth		
Vertical	$5.0 \times 10^{-14} \text{ m}^2 \text{ (50)}$	Initial Reservoir	102.5 °C	
Permeability	mD)	Temperature		
Thermal	2.1 W/m/°C	Injection	200 m	
Conductivity		Horizontal Well		
		Radius		
Porosity	10%	Production	707 m	
		Horizontal Well		
		Radius		
NaCl	20%	Number of grid	42	
Concentration		cells, vertical		
Geothermal	35 °C/km	Number of grid	117	
Gradient		cells, horizontal		
Reservoir Thickness	300 m			
Rock Density	2650 kg/m ³	Shallow		
		Reservoir		
Rock Specific Heat	1000 J/kg/°C	Mean Reservoir	1.5 km	
		Depth		
Simulated Radius	100 km	Initial Reservoir Temperature	67.5 °C	
Initial Conditions	Hydrostatic	Horizontal Well	400 m	
	equilibrium, pore	Radius		
	space occupied by	Number of grid	34	
	brine	cells, vertical		
Boundary	No fluid flow, semi-	Number of grid	121	
Condition Top/ Bottom	analytic heat transfer	cells, horizontal		
Boundary	No fluid or heat			
Condition	transfer			
Lateral				

vertical permeabilities of $5 \times 10^{-14} \, \mathrm{m}^2$ (50 mD) and a porosity of 10% as these are the base case conditions we have employed before, such as in [12,17,24,27,30]. The temperature of each reservoir is determined using a thermal gradient of 35 °C/km, resulting in an average reservoir temperature of 102.5 °C for the deep reservoir at 2.5 km depth and 67.5 °C for the shallow reservoir at 1.5 km depth, consistent with previous studies [12,48,49]. The initial reservoir pressure is determined using the hydrostatic pressure, resulting in initial pressures of 25 MPa and 15 MPa for the deep and the shallow reservoirs, respectively. Both reservoirs have a thickness of 300 m. The simulated reservoir radius is 100 km, consistent with previous models [24], to limit pressure boundary effects as the CO₂ plume size changes and as no-fluid-flow boundary conditions are applied on all sides. Additionally, the conductive heat flux across the top and bottom boundaries is modeled using a semi-analytic solution [45].

2.2.1.1. Deep reservoir. Geothermal heat is extracted from the deep reservoir which acts and the thermal energy source in CPG-F facilities. The deep reservoir has two horizontal wells: an injection well and a production well, shown in Figs. 1 and 2. The injection well is horizontal, located at the bottom of the reservoir at a radius of 200 m from the center axis and is connected to a single vertical injection well. This differs from previous work, which used a single vertical injection well with no horizontal component [12,24,26,29,50]. The injection well is located at the bottom of the reservoir to increase the volume swept by the CO₂ plume, as the CO₂ will buoyantly rise towards the caprock, extracting heat from the entire thickness of the reservoir. At the top of the reservoir, the CO2 accumulates beneath the caprock. The horizontal production well is located just beneath the caprock at a radius of 707 m, consistent with prior work [12,24-26,29], and the horizontal production well is connected to four vertical production wells, spaced equidistant along the horizontal well. Unlike a vertical production well, a horizontal production well under the caprock limits the brine produced with CO_2 as the entire well is in a CO_2 -rich location. Horizontal wells within the reservoir are used to reduce the overall reservoir pressure losses as a horizontal well is longer, has increased surface area, and thus can facilitate a lower mass flux.

To dry out the reservoir, it is assumed that CO_2 is continuously injecting for 2.5 years before any CO_2 is extracted from the reservoir for power production. Over this period, 15.8 Mt of CO_2 is injected into the reservoir that was initially filled with brine, consistant with previous studies [48]. After this volume is injected, the CO_2 gas saturation near the production well is over 30% and the wellbore CO_2 mass fraction is over 94%. A minimum 94% CO_2 mass fraction in the produced fluid was previously used as the allowable water content within CO_2 turbines [24,26,51].

2.2.1.2. Shallow reservoir. When the CPG-F facility is operated to provide energy storage, the shallow reservoir stores the CO_2 in between when power is produced and consumed. The reservoir has a single horizontal well, which functions as both the injection and production well. The single well limits the CO_2 plume advection and diffusion losses by keeping the CO_2 concentrated in a single area, allowing most of the injected CO_2 to be recovered later. The well is located beneath the caprock at a radius of 400 m. Similar to the deep reservoir, a horizontal well is used instead of a vertical well. Two vertical wells connect the surface equipment with the horizontal well.

The depth of the shallow reservoir is an important parameter for the performance of the system. The depth of the shallow reservoir must ensure that the CO_2 is in the supercritical state (7.38 MPa, i.e. reservoir depths exceeding 1 km), be shallower than the deep reservoir depth, and have a reservoir temperatures that is not suitable as a CPG system heat source (i.e. reservoir temperatures must be significantly below 100 $^{\circ}\text{C}$). Additionally, the depth of the shallow reservoir impacts the operation of the CPG-F system operating during energy storage; with deeper shallow reservoir depths increasing the amount of cooling that is required during the power generation mode, thereby decreasing the ability of the system to time-shift power dispatch and storage [49]. This limits the ideal depth of the shallow reservoir to between 1 km and 2 km in depth. Thus, a shallow reservoir depth of 1.5 km was selected for this study to maintain supercritical CO_2 conditions during the injection and production processes, and to reduce parasitic power losses during the power generation

The CO2 plume in the shallow reservoir is developed by injecting 0.67 Mt of CO₂ over 12 weeks, consistent with previous studies [48]. The pre-injection of CO2 into the shallow reservoir is used to displace the native brine and develop high CO2 saturations in the pore space surrounding the screen of the huff-and-puff combined injection-production well in the shallow reservoir (see also Fig. 1B). Sufficient pore-space CO₂ saturations surrounding a production well inlet enable the recovery of CO₂ from the reservoir with minimal uptake of native brine [28], reducing water extraction from the shallow reservoir. Low water extraction rates are important because any CO2-coproduced water or brine from the shallow reservoir has to be removed (and disposed of) before the CO₂ is injected into the deep reservoir as water injection into a reservoir reduces the fluid mobility and increases the fluid pressure near the deep injection well screen, reducing the well injectivity index and thus the injection well performance [24]. Unlike the deep reservoir, the shallow reservoir is designed to temporary store CO₂, not to extract heat, thus the swept volume by the CO₂ in the reservoir is minimized and much less CO₂ is used than in the deep reservoir. Additionally, the displacement of the native brine by the CO2 plume decreases the injection overpressure and the extraction pressure drawdown that occurs during the operation of the CPG-F system, as CO2 has a lower kinematic viscosity, experiencing lower pressure losses in the reservoir [49]. This also reduces the overall pressure losses in the shallow reservoir compared to the deep reservoir.

Consequently, the injection of 0.67~Mt of CO_2 was selected to limit the amount of CO_2 required for the shallow reservoir, while establishing the CO_2 saturation required for the injection/production operation. Increasing the mass of the injected CO_2 , while further displacing the brine from the combined injection-production huff-and-puff well, had little effect on the brine concentration in the produced CO_2 and the pressure drop that occurred between the fluid injection and production modes [49]. Decreasing the pre-injection CO_2 mass, increases the amount of water that is recovered and increases the fluid pressure drop between the injection and production modes (decreasing CPG-F power plant performance), due to brine encroachment on the well [49]. Injecting the CO_2 over a 12-week period was used to prevent large reservoir overpressures and reduce the amount of cooling that would be required during the power generation mode.

The shallow reservoir is designed to operate with minimal amounts of CO_2 ; however, diffusion and advection cause CO_2 to become inaccessible and lost to the surrounding reservoir over time [49]. To make up for these losses, only 98% of the injected CO_2 mass is produced each cycle. This provides a repeated resupply of CO_2 from the deep reservoir to the shallow reservoir and maintains the high saturation of CO_2 near the combined injection-production well in the shallow reservoir over the lifetime of the CPG-F system [49].

2.2.2. Power system modeling

The power system is comprised of the turbine, cooling towers, pump, throttling valve, and the vertical wells. The state points for the CPG-F facility are defined in Fig. 1 and the main surface plant parameters are given in Table 3. The surface power plants are simulated using Engineering Equations Solver (EES) with $\rm CO_2$ property relations from Span and Wagner [52]. The surface power plant component models are consistent with previous CPG power system models [12,40,48,49], discussed in detail in Fleming 2019 [49], and thus are only summarized below. The CPG-F power plant is assumed to be in a quasi-steady state for the analysis.

The vertical portion of the wells is numerically simulated using the well model of Adams et al. [12], using a steady state finite volume approximation, with the vertical wells subdivided into 100-meter elements. The model neglects fluid pressure losses in the horizontal wells within the reservoir. The model numerically integrates across each element (i.e. from state i to state i+1), starting with the reservoir state (State 1), which is determined from the subsurface reservoir model, to the surface. Across each element, the energy balance equation (Equation (1)), momentum equation (Equation (2)), and continuity equation (Equation (3)) are solved simultaneously (for variable definitions, see Table 1).

$$h_i\left(\frac{10^3 \text{J}}{1 \text{kJ}}\right) + gz_i = h_{i+1}\left(\frac{10^3 \text{J}}{1 \text{kJ}}\right) + gz_{i+1}$$
 (1)

$$P_{i}\left(\frac{10^{3}\text{Pa}}{1\text{kPa}}\right) + \rho_{i}gz_{i} = P_{i+1}\left(\frac{10^{3}\text{Pa}}{1\text{kPa}}\right) + \rho_{i+1}gz_{i+1} - \Delta P_{loss}\left(\frac{10^{3}\text{Pa}}{1\text{kPa}}\right)$$
(2)

Table 3Parameters used for the surface power plant simulations.

Parameter/Value	
Surface Wet Bulb Temperature	15 °C
Vertical Well Inner Diameter	0.41 m
Vertical Well Surface Roughness	55 μm [53]
Deep Reservoir Vertical Production Wells	4
Deep Reservoir Vertical Injection Wells	1
Shallow Reservoir Vertical Wells	2
High-pressure Turbine Backpressure	7.5 MPa
Turbine Isentropic Efficiency	78%
Pump Isentropic Efficiency	90%
CPG Condensing Tower Approach Temperature	7 °C
CPGES and CPG + CPGES Condensing Tower Approach	7 °CT ₁₁ -
Temperature, lesser of	15 °C

$$\dot{m} = \rho_i A V_i = \rho_{i+1} A V_{i+1} \tag{3}$$

The well is assumed to be adiabatic and neglects kinematic energy [12,13]. The frictional pipe losses are modeled using the Darcy–Weisbach relation (Equation (4)), where the friction factor is determined from the moody chart [54] using a surface roughness, ϵ , of 55 μ m, based on bare Cr13 oil piping [53].

$$\Delta P_{loss} = f \frac{L_{pipe}}{D} \rho \frac{V^2}{2} \left(\frac{1 \text{kPa}}{10^3 \text{Pa}} \right) \tag{4}$$

A well diameter of 0.41 m is used to reduce the pressure losses in the well, which can be significant. Small well diameters significantly reduce power output and several simulations have shown that larger pipe diameters can be a cost minimization strategy [11,12,40]. However, smaller pipe diameters may also reduce costs by reducing the heat extraction rate from a reservoir, thereby reducing the required capacity of the power plant at the land surface and increasing its utilization, resulting in reduced power generation costs [30]. The CPG-F system has seven vertical wells (Fig. 2), the five deep reservoir vertical wells (one injection, four production) plus two vertical (huff-and-puff) wells to the shallow reservoir. Once at the reservoir, the vertical wells connect to the horizontal collection wells described in previous sections.

The power produced from the turbine is calculated using the mass flow rate and the enthalpy difference across the turbine using an isentropic efficiency of 78%. The high-pressure turbine (HPT) backpressure for the system is 7.5 MPa (State 3) to provide sufficient pressure to overcome CO2 injection into the shallow reservoir and to maintain the CO₂ supercritical, preventing multiphase flow in the vertical well (State 8). The system operates with a low-pressure turbine (LPT) backpressure of 6.0 MPa (State 4), the saturation pressure for CO₂ at a temperature of 22 °C that is set by State 5, the saturated liquid condition at the exit of the condensing tower. The condensing pressure for the energy storage configuration (State 4) is equivalent to the shallow reservoir wellhead pressure (State 11). A CPG-F facility cannot operate when the wellhead temperature (State 11) is less than the ambient temperature (15 °C) as heat rejection (and thus the phase change of the CO₂ from the gas to liquid) cannot occur. In these cases, values were omitted from the figures and tables.

A CPG-F facility may use an isenthalpic throttling valve to reduce the shallow reservoir wellhead pressure (State 11) to the condensing pressure (State 4) of $\rm CO_2$ at a temperature of 22 °C (5.4 MPa), when the system is operated to provide dispatchable power and energy storage simultaneously (Section 3.5). If the shallow reservoir production temperature is below 22 °C, but above 15 °C, no throttle is used and the condensing pressure is reduced to the wellhead pressure (State 11), thereby reducing the approach temperature (see Table 3) and the condensing tower outlet temperature (State 5).

The components that consume power are the pumps and the cooling towers. Pumps are used to increase the fluid pressure at the land surface before the fluid is injected into the deep reservoir. The power that is used by a pump is calculated by the mass flow rate times the change in enthalpy across the pump, using an isentropic efficiency of 90%. The cooling towers consume parasitic power to operate the fans which reject heat from the $\rm CO_2$ to the surrounding atmosphere. The parasitic power consumption for the cooling towers is modeled as a fraction of the total heat rejection, given as

$$\dot{W}_{CoolingTower} = \lambda \dot{Q}_{CoolingTower} \tag{5}$$

where λ is the parasitic loss fraction, which is a function of the cooling tower approach temperature and the ambient wet bulb temperature, as defined in Adams et. al [12], and the heat transfer rate is defined as the mass flow rate times the enthalpy difference across the cooling tower.

For the CPG-F dispatchable power system, the net power is the sum of the turbine power, cooling tower power, and pump power (Equation

(6)). The cooling tower power and pump powers are parasitic powers and are, therefore, negative.

$$\dot{W}_{CPG,net} = \dot{W}_{CPG,turbine} + \dot{W}_{CPG,cooling} + \dot{W}_{CPG,pump} \tag{6}$$

For the CPG-F designed for energy storage, the generation power is the sum of the turbine power and the (zero or negative) shallow reservoir pre-injection cooling tower power (Equation (7)).

$$\dot{W}_{CPG-F,generation} = \dot{W}_{CPG-FS,turbine} + \dot{W}_{CPG-F,cooling,generation} \tag{7}$$

Similarly, the storage power is the sum of the cooling tower power and the pump power, both of which are zero or negative (Equation (8)).

$$\dot{W}_{CPG-F,storage} = \dot{W}_{CPG-F,cooling,storage} + \dot{W}_{CPG-F,pump}$$
 (8)

The generation and storage powers of the CPG-F system change over the generation or storage period as the reservoir pressures change. When a single value is reported to represent an entire period, it is a timeaveraged value.

The energy is the integral of the power over time. The energies of the CPG and the CPG-F systems are given in Equations (9) through (12).

$$W_{CPG,net} = \int_{0}^{24h} \dot{W}_{CPG,net} dt \tag{9}$$

$$W_{CPG-F,generation} = \int_{0}^{t_{generation}} \dot{W}_{CPG-F,generation} dt$$
 (10)

$$W_{CPG-F,storage} = \int_{t_{annearism}}^{24h} \dot{W}_{CPG-F,storage} dt$$
 (11)

$$W_{CPG-F,net} = W_{CPG-F,generation} + W_{CPG-F,storage}$$
(12)

In the modeling for this study, a CPG-F facility operates continuously for 24 h when only dispatchable power is provided. In contrast, when operating to provide other services, the facility may produce power for only a portion of a 24-hour period. The ratio of the electricity generation time to total operation time is the duty cycle, given in Equation (13).

$$DutyCycle = \frac{t_{generation}}{24 \text{hours}} \tag{13}$$

For this analysis, four duty cycles were selected for production periods of 16h, 12h, 8h, and 4h. These are respectively labeled: "16h-8h", "12h-12h", "8h-16h", and "4h-20h," also shown in Table 4.

The CO₂ stream is split when the CPG-F facility operates to provide both dispatchable power and energy storage and the ratio of the dispatchable power CO₂ mass flow rate divided by the total CO₂ mass flow rate used to make power is the split mass fraction, mf_{split} (Equation (14)).

$$mf_{split} = \frac{\dot{m}_{dispatchable}}{\dot{m}_{dispatchable} + \dot{m}_{energystorage}}$$
(14)

The facility can operate with mass fractions from 0% (0% dispatchable and 100% energy storage) to 100% (100% dispatchable and

Table 4Duty cycles examined in this study.

Duty Cycle	Cycle Parameter	Cycle Characteristics
16h-8h	16-hour power production followed by 8-hours of power consumption	Peaking power consumption with extended power production
12h-	12-hour power production	Balanced power production and
12h	followed by 12-hours of power consumption	consumption
8h-16h	8-hour power production followed	Moderate peaking power
	by 16-hour of power consumption	production with extended power consumption
4h-20h	4-hour production followed by 20-hour of power consumption	Full peaking power production with extended power consumption

0% energy storage). For this analysis, five energy storage mass fractions (mf_{energy storage}) were chosen: 0%, 25%, 50%, 75%, and 100%. Mass flow rates, and daily circulation rates are calculated using the same method as prior work [49]. All mass flow rates are provided is the supplemental information (Table S1, S2).

2.3. Cost estimation

The capital costs of the CPG-F facility are calculated with genGEO capital cost model [55]. The capital cost consists of three components: reservoir and monitoring wellfield development, geothermal wells, and surface power plant. The geothermal wells and wellfield costs are fixed for all sizes of surface equipment and mass flow rate. Conversely, the surface plant has no fixed cost and varies exclusively with equipment (turbine, pump, and cooling tower) size and flow rate. In all cases, greenfield development costs are used, and all costs are overnight values in United States dollars (USD) for 2019. Assuming brownfield development (i.e. an existing CO₂ sequestration site with adequate injection wells) would substantially reduce costs, but would be an optimistic assumption. The reservoir development cost model includes the site characterization, leasing, tracer tests, stimulation, air and groundwater monitoring equipment, stratigraphic wells, and monitoring wells. No cost or credit for acquiring the CO₂ is considered.

The specific capital cost, SCC [\$/MW], of the system is the total project capital cost, divided by the power generation capacity of the system. The specific capital cost of the facility as a power capital cost (\$/MW) is reported instead of other cost metrics, such as the levelized cost of electricity, or levelized cost of storage, to avoid using financing assumptions. In addition to the power capital cost, energy storage technologies are also described with an energy capital cost (\$/MW-h), which takes into account the length of time energy can be stored or discharged. This metric does not apply as cleanly to CPG-F facilities designed to provide energy storage as other energy storage approaches (e.g., batteries) because the energy storage occurs in the reservoir and thus the length of time a CPG-F facility can dispatch and store electricity is more of an operator decision than a system constraint. In other words, the energy capital cost of a CPG-F facility designed to provide energy storage over any duration, could be thought of as being \$0/MW-h because it does not change capital costs to increase or decrease the hours of energy stored. At the same time, the size of the surface equipment (e. g., turbine), and thus the specific capital cost, could change for a facility designed to provide energy storage over a specific duration compared to another (e.g., 16h-8h vs 12h-12h). As a result, the total capital cost [\$] of the CPG-F facility is reported instead of the specific capital cost in some situations for simplicity.

3. Results and discussion

Here, CPG-F facilities, designed to provide different services, are characterized in terms of the net daily energy production, power production, power storage, and cost. The complete results are in tables in the appendix. The results presented here are for a single day after 10 years of continuous operation once the $\rm CO_2$ injection and production pressures have stabilized. At some elevated $\rm CO_2$ circulation rates (flow rates exceeding 20kt/day for the 4h-20h duty cycle, and 40 kt/day for the 8h-16h and 16h-8h duty cycles), the wellhead temperature of $\rm CO_2$ extracted from the shallow reservoir is below the minimum temperature (i.e. the ambient wet bulb temperature) necessary to reject heat from the $\rm CO_2$. In these high flowrate cases, a solution cannot be found, and no value is reported.

A standard CPG power plant, without the addition reservoir (i.e., not CPG-F), is modeled for the given reservoir to provide a reference point for CPG-F simulations. Thus, a brief description of the CPG results is provided (section 3.1). The results of a CPG-F facility designed for energy storage are provided as a function of duty cycle and $\rm CO_2$ production flow rate (section 3.2), followed by design cases determined based on

optimal flow rates (section 3.3). The cost of designing a CPG-F facility that can operate across all duty cycles and flowrates is discussed in section 3.4. Lastly, a CPG-F facility designed to provide both dispatchable power and energy storage simultaneously is discussed in section 3.5.

3.1. CPG power plant results

The amount of power, and thus energy, produced by the CPG power plant varies with the mass flow rate, shown in Fig. 3. As the mass flow rate increases the turbine produces more power. However, the pressure losses within the reservoir and surface piping also increase with mass flow rate, decreasing the pressure differential across the turbine and increasing the amount of pumping required. This turbine pressure reduction counteracts the turbine output gains due to increased mass flow rate and results in maximums in both the net power and energy. For the system parameters (e.g. reservoir depth, temperature, permeability) considered here and shown in Fig. 3, the optimal mass flow rate which provides the most power and energy is 39 kt/day (450 kg/s). At this mass flow rate, 60 MWe-h of energy is produced per day at a continuous rate of 2.5 MWe-

The specific capital cost of a CPG power plant is also shown in Fig. 3. As an alternative to selecting a $\rm CO_2$ mass flow rate to maximize net power, a flow rate can be chosen to minimize the specific capital cost. Thus, a CPG power plant has at least two optimal mass flow rates: 1) for maximum net power production, and 2) for minimum specific capital cost, the latter of which has not been considered previously [10,11]. Here, the minimum specific capital cost occurs at a mass flow rate of 35 kt/day (400 kg/s), while the maximum net power occurs at a mass flow rate of 39 kt/day (450 kg/s). Operating at the minimum specific capital cost mass flow rate produces 2.49 MWe, or 59.7 MWe-h/day, which is 99% of the power/energy when operating at the maximum net energy flow rate, but at 98.6% of the specific capital cost. Thus, in this scenario, the two operational points are very similar.

This work continues to determine the power production at the mass flow rate of maximum power production, which is consistent with previous analyses [12]. Future work may include operating a CPG power plant at a flow rate which minimizes specific costs.

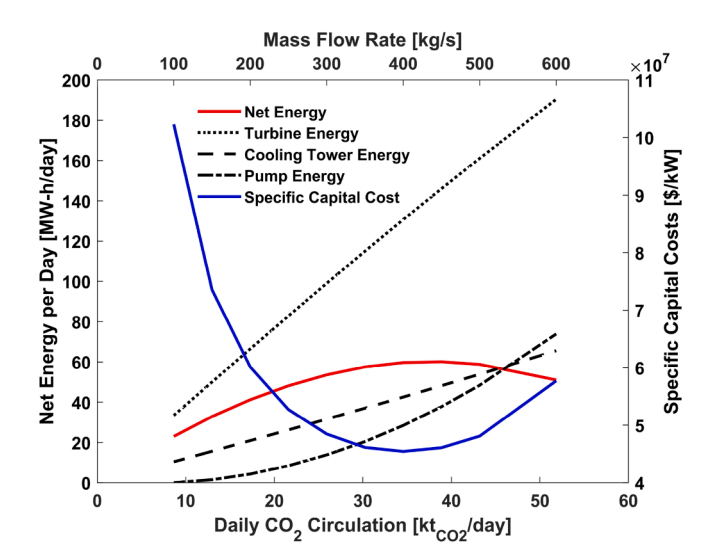


Fig. 3. The daily energy production and consumption for major system elements and the specific capital costs for a CPG power plant. Net power production is maximized at a $\rm CO_2$ mass flow rate of 39 kilotonnes per day (450 kg/s), while specific capital costs are minimized at a $\rm CO_2$ mass flow rate of 35 kilotonnes per day (400 kg/s).

3.2. CPG-F designed for energy storage duty Cycles: Variations in daily CO₂ circulation

Fig. 4A shows that a CPG-F facility designed for energy storage has a circulation rate that delivers maximum power. This is due to the relationship between the turbine power production and the parasitic power consumption of the cooling towers, similar to the maximum in a CPG power plant, discussed previously. Additionally, Fig. 4A shows that for the same $\rm CO_2$ circulation rate, the production power is higher for short production periods (e.g. 4h-20h duty cycle) than for longer production

periods due to the higher production period CO_2 mass flow rate for the same rate of daily CO_2 circulation.

Fig. 4B shows that storage power, which consists of parasitic powers and is therefore a proxy for system losses or inefficiencies, becomes large at high storage mass flow rates. For a given daily $\rm CO_2$ circulation rate, a duty cycle with a shorter storage period (e.g. 16h-8h) will have a higher storage mass flow rate than a duty cycle with a longer storage period (e.g. 4 h-20 h). Thus, duty cycles with shorter storage periods (e.g. 16h-8h) have higher power consumption for a given $\rm CO_2$ circulation rate than those with longer storage periods.

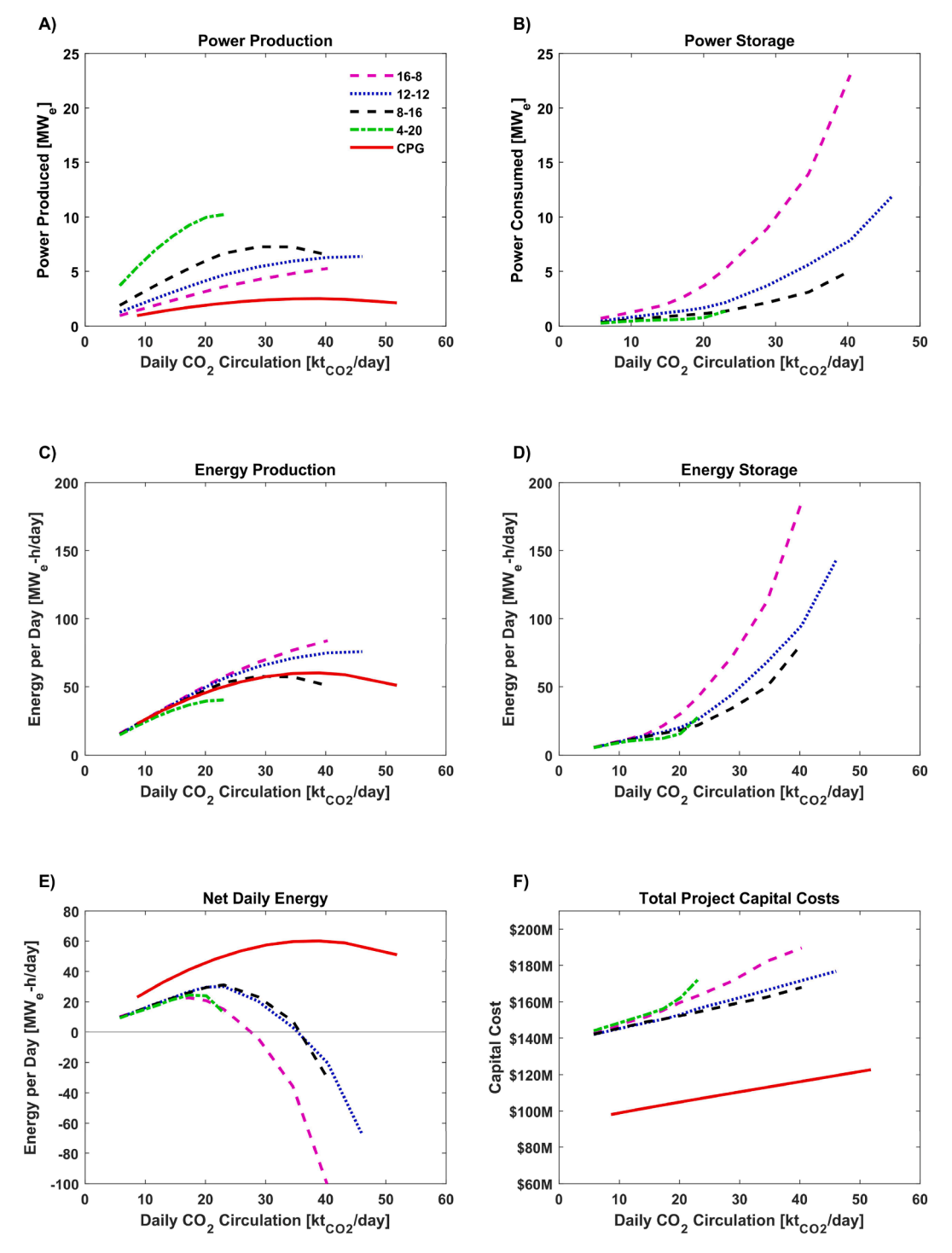


Fig. 4. The performance metrics of CPG-F facilities designed for energy storage and a CPG power plant for varying CO₂ circulation rate: A) the power production, B) the power consumption during the storage mode, C) the energy produced during the production mode, D) the energy consumed during the storage mode, E) the net daily energy produced, and F) the total project capital cost.

Fig. 4C and Fig. 4D show the energy produced and stored over a 24hour period. Fig. 4C shows that the electricity generation energy is similar to, or slightly larger than, the CPG power plant net energy. Thus, a CPG-F facility designed for energy storage can produce approximately the same energy as a CPG power plant, but in a smaller window of time. The energetic cost of this increased power availability is shown in Fig. 4D, wherein the CPG-F facility energy storage curves increase polynomially with flow rate, but a CPG power plant has no storage energy. This results in a CPG power plant generating the greatest net daily energy, shown in Fig. 4E. This is expected, as the CPG-F facility designed for energy storage eliminates the low-pressure turbine (Fig. 1) and its corresponding energy production to incorporate the shallow reservoir and add energy storage capability. Thus, the CPG power plant and CPG-F facilities designed for energy storage naturally fall into separate groups in Fig. 4E. Additionally, there are less energy efficient duty cycles than others, particularly at larger daily circulation rates. Both the 4h-20h duty cycle and 16h-8h duty cycle have substantially less net daily energy due to their imbalance of production and storage mass flowrates, discussed previously.

Fig. 4F shows the total project capital cost for both a CPG power plant and a CPG-F facility designed for energy storage. The systems have different costs for two primary reasons: CPG-F facilities need 1) the additional reservoir, geothermal wells, and monitoring wellfield and 2) increased surface equipment. The well and wellfield costs shift the CPG-F facility cost curves up by a fixed value of \$43.4 M. The equipment costs tend to both shift the cost upwards and increase with daily circulation rate. The upward shift in equipment cost is due to the intermittent operation of the equipment. For example, if the 12h-12h system operates at the same CO2 daily circulation rate as a CPG power plant, the production and storage mass flow rates will need to be double the flow rates of the CPG power plant, and therefore the equipment (e.g. turbine and cooling tower) both have to be twice as large. Additionally, the increase in equipment cost with daily circulation rate is due to the growing inefficiencies (pipe and reservoir friction losses) at large flow rates and their associated parasitic powers. In general, the reservoir accounts for over 85% of the pressure loss, but at the largest flow rates in the energy storage configuration, the well pressure losses (mainly the deep injection well) can exceed 20% of the total pressure loss. Thus, a CPG power plant has the lowest capital costs and the highest daily average energy. Conversely, the CPG-F facility here has up to 310% more production power than the CPG power plant at the expense of system inefficiency and capital costs. However, either option may be financially viable depending on the value of the services provided and the market incentives to provide those services.

$3.3.\ \ CPG-F$ designed for energy storage duty Cycles: Optimal flow rate design points

So far, the operation of CPG-F facilities designed for energy storage has been shown with respect to the daily CO_2 circulation rate, or average daily mass flow rate. The mass flow rate is a design condition which is chosen by the system engineer, i.e. it is an input to the system. In the CPG power plant analysis (Section 3.1), it was demonstrated that the mass flow rate can be chosen to maximize power (and thus energy), as done in previous studies [12,29], or to minimize the specific capital cost.

A similar approach to CPG-F facilities, designed to provide energy storage, was applied, however, the variable nature of providing energy storage and the market needs, which the CPG-F facility needs to meet, are different than for CPG power plants, so that multiple design point mass flow rates are possible. Therefore, four potential mass flow rate operational cases for CPG-F facilities, designed to provide energy storage, are defined:

• Case 1: Maximum Daily Net Energy: The facility delivers the largest net energy to the grid over a complete daily cycle. This is similar to the design point for the CPG power plant.

- Case 2: Maximum Power: The facility delivers the maximum possible power during the production mode, despite the large energy penalties during the storage mode.
- Case 3: Zero Daily Net Energy: The facility produces and stores energy such that the net is zero. This usually provides an operational point between Cases 1 and 2. This operation is similar to an ideal battery with a round-trip efficiency of one.
- Case 4: Minimum Specific Capital Cost: The facility operates so that the specific capital cost of power production is minimized.

Fig. 5A through 5D show the dependency of energy and cost on the ${\rm CO}_2$ circulation rate. For each duty cycle, the operational points for Cases 1 through 4 are shown with a numbered vertical line. The daily circulation for each of the optimized cases was determined directly using the simulation data for maximum daily net energy, maximum power, and minimum specific capital cost cases. The zero daily net energy case is determined by linear interpolation of the data.

The Case 1 (Maximum Daily Net Energy) operational point occurs at the lowest daily circulation rates for all duty cycles. While this design point balances the net energy production with the parasitic losses for a CPG power plant, it generally limits the amount of power dispatched and stored from a CPG-F facility designed for energy storage, and thus should only be considered as a lower bound design point.

The Case 2 (Maximum Power) operational point tends to occur at large daily circulation rates, but this can vary depending on the duty cycle. As discussed earlier, the net production energy delivered to the grid will always theoretically reach a maximum after which pressure losses reduce energy output; however, this maximum is not always observed. For example, in Fig. 5A, the temperature of CO₂ produced (State 11 in Fig. 1) during the storage period above 40 kt/day is below the ambient temperature at the surface; therefore, heat can no longer be rejected, and the system simulation cannot be solved. Thus, no results, including a maximum in energy production, are reported above 40 kt/day for the 16h-8h duty cycle, 46 kt/day for the 12h-12h duty cycle, and 23 kt/day for the 4h-20h duty cycle. Additionally, the Case 2 operational points can have very large, negative net daily energy as these points occur at high flowrates which have large storage period energy consumption.

The Case 3 (Zero Net Daily Energy) operational points tend to be a compromise between those of Cases 1 and 2, providing increased production power but without the increasing inefficiency that occurs at large mass flowrates. The Case 3 point has equal parts energy production and storage, thus, this scenario can be best compared to traditional energy storage technologies (e.g. pumped-hydro or batteries). In some duty cycles with long storage periods (i.e. 8h-16h and 4h-20h), the Case 3 operation point occurs at higher daily circulation rates than Case 2. When this occurs, the production power and the daily net energy decrease from Case 2, and there is no practical application for Case 3 in these duty cycles.

The Case 4 (Minimized Specific Capital Cost) operational points occur at flow rates greater than those of Case 1 (Maximum Daily Net Energy) but equal to or below Case 2 (Maximum Power). Similar to Case 3, the minimum specific capital cost is a compromise between high power production and large net daily energy production.

Fig. 6 shows the power production and net daily energy production for a CPG power plant and a CPG-F facility designed for each energy storage duty cycle and four flow rate cases. All the CPG-F energy storage design cases considered deliver more power than the CPG power plant. For a given duty cycle, there is no apparent advantage to operating at circulation rates lower than those specified by Case 1 or greater than that of Case 2. If the flow rate is reduced below that of Case 1 (maximum net daily energy), both the power and energy decrease while the specific capital cost increases. Similarly, circulation rates greater than Case 2 will decrease production power and net daily energy while specific capital costs increase.

The 8h-16h and 4h-20h duty cycles both provide positive net daily

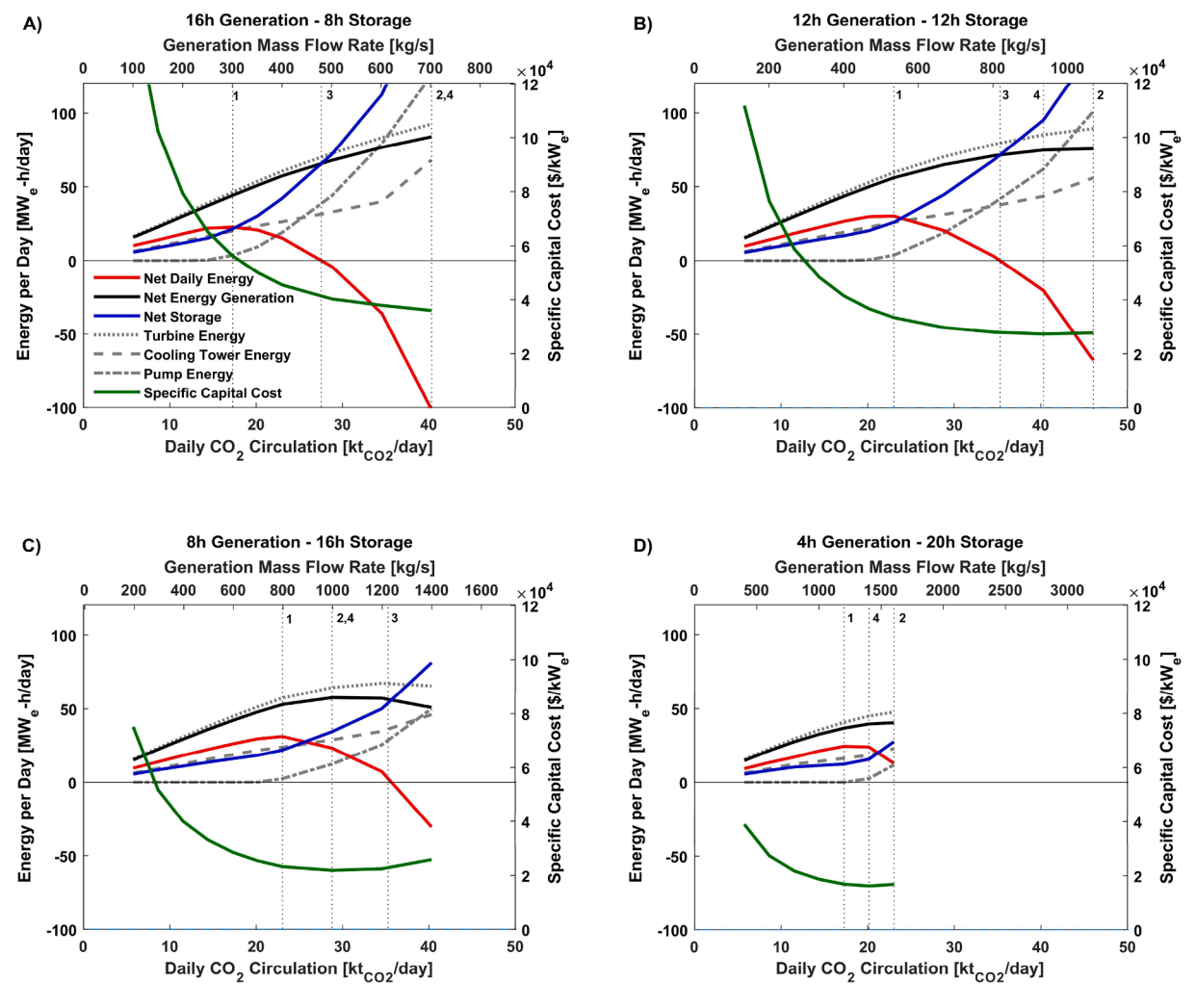


Fig. 5. Energy and cost values of a CPG-F facility designed for four different energy storage duty cycles: the A) 16 h-8 h case, B) 12 h-12 h case, C) 8 h-16 h case, and D) 4 h-20 h case. The daily CO_2 circulation is marked for each of the following cases: Case 1) maximum daily net energy, Case 2) the maximum power production, Case 3) zero daily net energy, and Case 4) the minimum specific capital cost.

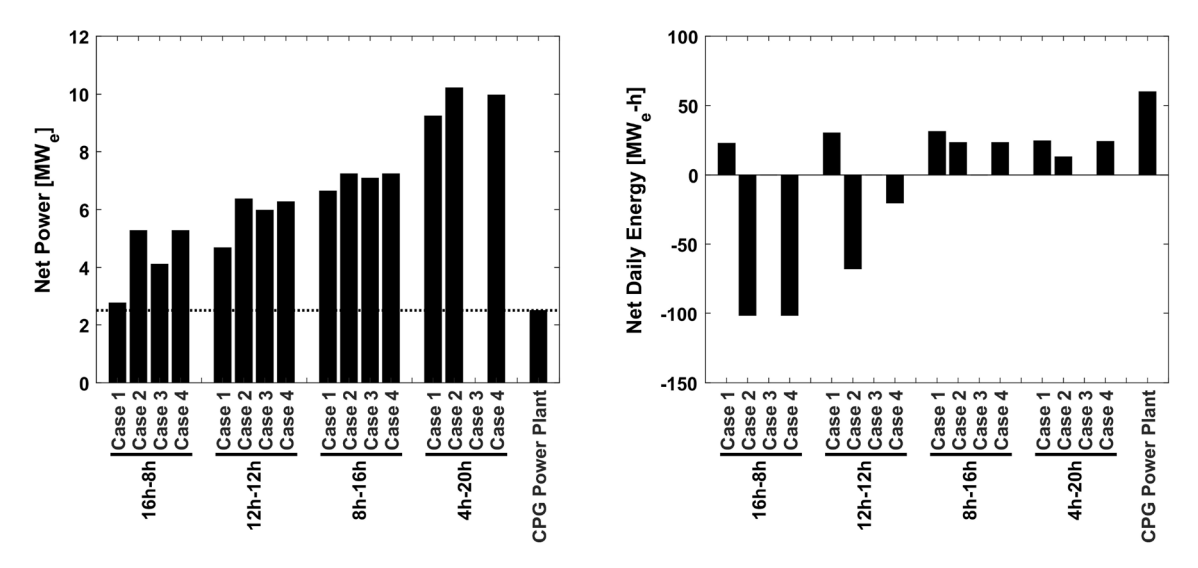


Fig. 6. The A) net production power and B) net daily energy of a CPG power plant and a CPG-F facility designed for different energy storage duty cycles and operational flow rate cases.

energy while also providing the highest production power. This is due to their long storage periods with corresponding low storage mass flow rates. As previously noted, large pump powers occur at high storage mass flow rates and are a primary driver for large storage energy, and thus negative net energy for a complete cycle.

Therefore, our general finding is that CPG-F facilities designed for energy storage will tend to have fewer inefficiencies, higher net energy, and increased power production if operators adopt a strategy which provides slower, more consistent injection into the deep reservoir. This is also the reasoning for designing a CPG-F facility to provide both dispatchable power and energy storage simultaneously (described in section 3.5), whereby partial continuous injection reduces the average flowrate into the deep reservoir.

3.4. CPG-F designed for any energy storage duty Cycle: Cost

The capital cost breakdown for each of the CPG-F facilities from the previous section is compared with the breakdown for CPG power plant in Fig. 7. The largest costs in all cases are the geothermal wells and well drilling costs, which are fixed at \$105 M for CPG-F facilities. This cost ranges from 56% to 74% of the total project capital cost, but on average is 68%. The reservoir configuration chosen here uses horizontal wells which provide large power output but adds substantially to the cost. Future work may optimize length of well drilled to balance power production and cost. Aside from the geothermal well and drilling costs, the next largest costs tend to be the monitoring wells and reservoir exploration costs, which are both fixed for CPG-F facilities. When these costs are combined with the geothermal well and drilling costs, the cost to find, assess, and access the geothermal sources for CPG-F facilities is \$132 M, or on average 85% of the total project capital cost.

The CPG power plant in Fig. 7 costs \$115 M, while most of the CPG-F facilities cost between \$154 M and \$190 M. Thus, in the cases considered, CPG-F facilities designed for energy storage can reasonably cost between 34% and 65% higher than CPG power plants.

Thus far, power, energy, and cost for each of the four duty cycles and the four cases have been reported (i.e. daily circulation rates). However, it is very likely that a CPG-F facility designed for energy storage will not be permanently operated at any one duty cycle and flow rate, but rather vary its operation based on the electrical grid demand and market conditions. For example, on peak demand days, the system may operate at the 4h-20h Case 2 condition, while it may operate in a 12h-12h Case 3

condition on other days. Thus, a CPG-F facility designed to provide energy storage across all duty cycles and cases was investigated. Here, this "any duration" CPG-F facility is only defined by the size of the power equipment (i.e. turbine, cooling tower, and pump) required to provide adequate capacity for all the defined operational conditions.

Fig. 7 shows the cost breakdown for the CPG-F facility that operates over all cycles (16h-8h to 4h-20h) and cases examined (i.e. Cases 1 to 4). For such a system that can operate over all cycle durations, the components (e.g. turbine, cooling tower, pump) are of the maximum size required for the underlying simulations, and these sizes are used to determine the total surface plant cost. Thus, designing a CPG-F facility to provide energy storage across varying duty cycles requires oversizing the components for most operating cycles and cases. Such an "any duration" system costs \$196 M, which replaces a range of systems that cost from \$154 M to \$190 M. Additionally, Fig. 6 shows that this "any duration" CPG-F facility can produce between 4.7 MWe and 10.2 MWe, compared to 2.5 MWe produced with a CPG power plant. Thus, the cost of a flexible system, which can produce 90% to 310% more power than a CPG power plant, is 4% to 27% higher than most duty-cycle-specific CPG-F facilities and 70% higher than a CPG power plant.

3.5. CPG-F system designed to simultaneously provide dispatchable power and energy storage

In this section the operational capabilities of CPG-F facility are combined to provide both dispatchable power and energy storage simultaneously. This allows for continuous, dispatchable net energy production and periodic additional (peaking) power production and storage. Designing a CPG-F facility in this way adds flexibility in operation to meet the fluctuating electricity grid demands.

For this analysis, it is assumed that the energy storage portion of a CPG-F facility operates on an 8h-16h duty cycle, however, any of the duty cycles could have been chosen. The system is simulated at five daily mass fractions (equation (14)), specifically: "100% dispatchable", "75% dispatchable + 25% energy storage", "50% dispatchable + 50% energy storage", "25% dispatchable + 75% energy storage", and "100% energy storage". For this section, a combined daily $\rm CO_2$ circulation rate of 34.6 kt/day was selected, the circulation rate for minimized specific capital cost for CPG-F facilities, designed to only provide energy storage (also near the maximum power production for that design).

Fig. 8 shows the combined power produced from a CPG-F facility

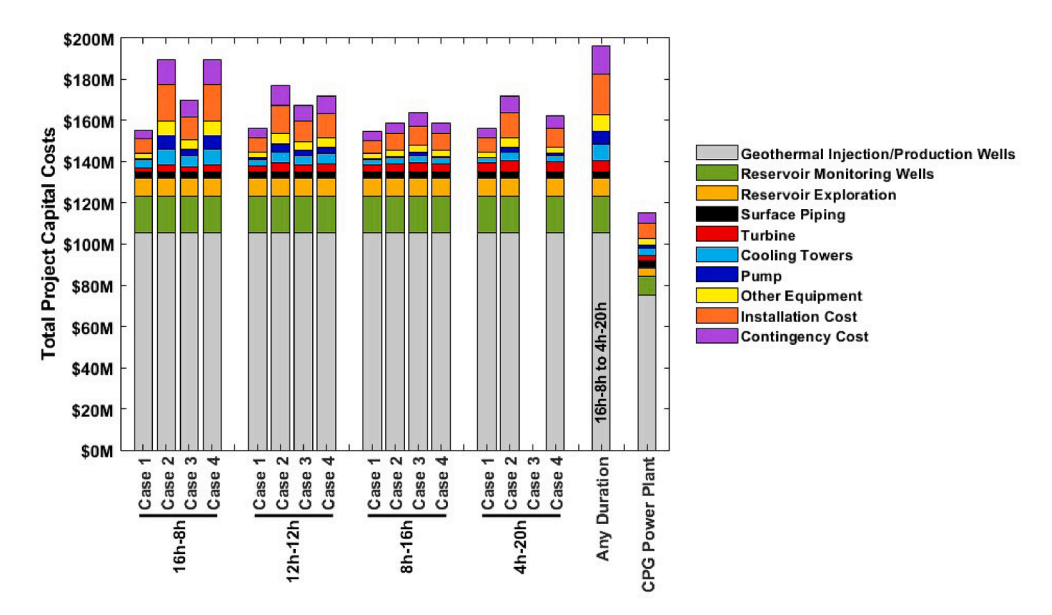


Fig. 7. The cost breakdown for each of the CPG-F facility designs for energy storage considered in this study. The vertical well costs represent approximately two thirds of the total capital costs. The "16 h-8 h to 4 h-20 h" flexible system can operate during most duty cycles and cases while costing 4% to 27% more.

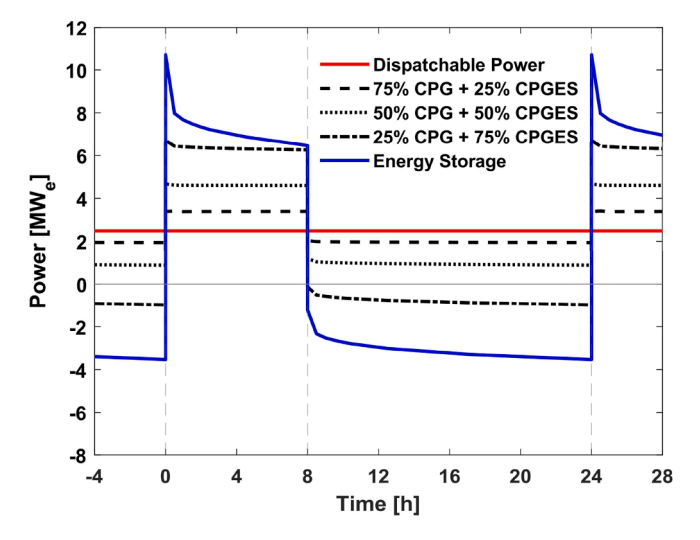


Fig. 8. The net power produced and consumed over a complete diurnal cycle for CPG-F operating to provide both dispatchable power and energy storage simultaneously, including the CPG and CPG-F designed for only 8 h-16 h energy storage duty cycle. All results are for a daily CO₂ circulation rate of 34.6 kt/day.

during a 24-hour period. The first eight hours is the production period, followed by the storage period for the remaining 16h. Note, the term "storage period" is used here to be consistent with the terminology from earlier sections; however, this may be confusing as the facility still

supplies net power to the electrical grid during most storage periods.

In Fig. 8, the 100% dispatchable power output is a horizontal line of 2.5 MW $_{\rm e}$. As the operational combination shifts from "100% dispatchable" to "75% dispatchable + 25% energy storage", the output during the production period increases to 3.4 MW $_{\rm e}$ and drops to 2.0 MW $_{\rm e}$ during the storage period. At a mass fractions of "25% dispatchable + 75% energy storage" and "100% energy storage," the storage period power output is negative, and power is removed (i.e. stored) from the grid. Thus, in this variable, the power output can be adjusted throughout the day to meet demand while still continuously generating power to maximize revenue.

Fig. 9 shows the CPG-F facility power, daily net energy, and cost for multiple flow rates. Generally, adding some dispatchable production functionality to the facility designed to only provide energy storage increases the daily net energy but decreases the peak production power. For example, Figs. 8 and 9A shows that shifting from "100% energy storage" to "25% dispatchable + 75% energy storage" for a CO $_2$ circulation rate of 34.6 kt/day decreases the average production power from 7.2 MW $_{\rm e}$ to 6.4 MW $_{\rm e}$, or -11%. At the same time, Fig. 9B shows the daily net energy increases by 431% from 7.2 MW $_{\rm e}$ -h to 38.2 MW $_{\rm e}$ -h. Thus, by designing a CPG-F facility to provide both dispatchable power and energy storage, the daily net energy increases at the expense of power production, when compared to a CPG-F system designed to only provide energy storage.

In some cases, designing a CPG-F facility to provide both services simultaneously can increase both the power production and daily net energy, compared to a system designed for only energy storage. For example, in Fig. 9A for daily CO_2 circulation rates above 40 kt/day, the

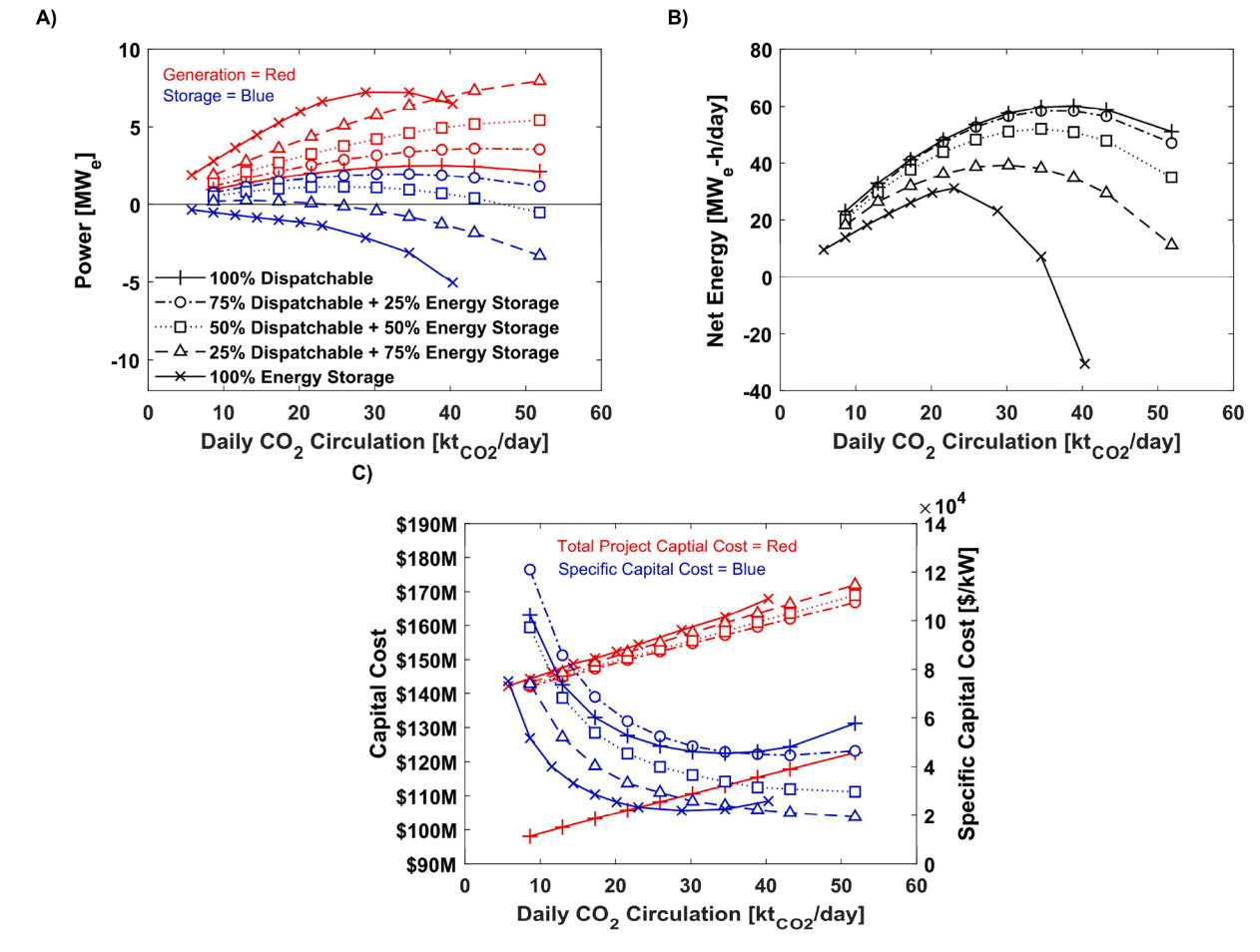


Fig. 9. The performance of a CPG-F facility designed to provide both dispatchable power and energy storage simultaneously, compared to a CPG power plant and a CPG-F facility designed to provide only energy storage over a 8 h-16 h duty cycle in terms of A) the power produced during the production and recharge modes, B) the daily net energy, C) the total and specific capital costs.

"25% dispatchable + 75% energy storage" system produces more power than the "100% energy storage" system alone. This phenomenon is a result of distributing the $\rm CO_2$ amongst multiple pathways in the system, allowing them all to operate more efficiently. For example, at a daily $\rm CO_2$ circulation rate of 40 kt/day, the 100% energy storage produces mass flow rate is 1400 kg/s. At that same daily circulation rate, the "25% dispatchable + 75% energy storage" system has a dispatchable production mass flow rate of 233 kg/s and an energy storage mass flow rate of 700 kg/s. As a result, both reservoirs have reduced injection and production mass flow rates, and the system operates with fewer pressure losses and higher storage efficiency. Thus, Fig. 9 shows the "25% dispatchable + 75% energy storage" system produces about the same production power at 43 kt/day as the 100% energy storage system does at 29 kt/day, but with 27% more daily net energy.

Fig. 9C shows that despite the variation in operation, a CPG-F facility designed for only providing energy storage over an 8h-16h duty cycle and a CPG-F facility designed to provide both services simultaneously have similar costs. The capital cost of a CPG-F facility designed to provide both services simultaneously are offset from the CPG power plant by a nearly constant value, which is primarily the cost of the shallow reservoir and the additional wells.

A CPG-F facility designed to provide both services simultaneously extends the maximum daily circulation rates beyond the useful values for either "100% dispatchable" or "100% energy storage." Fig. 9A shows that a CPG-F facility designed for both services all have maximum production powers at CO $_2$ circulation rates higher than the CO $_2$ circulation rate of 39 kt/day that maximized energy for CPG power plants. However, in Fig. 9B, the daily net energy maximums of the CPG-F facilities designed for both services all occur between the "100% energy storage" and the "100% dispatchable" daily net energy maximums, both in terms of energy production and the daily CO $_2$ circulation rate. Thus, while a CPG-F facility designed for both services can increase and extend the power that is produced, the net energy production is always bounded by the "100% energy storage" and "100% dispatchable systems."

In Section 3.4, the cost of an "all duration" CPG-F facility designed to provide only energy storage across all duty cycles and flow rates was found. The same approach is taken here, but for a CPG-F facility that is designed to provide anywhere between 100% dispatchable power and 100% energy storage. To do this, the maximum cost of each component (i.e. turbine, pump) is summed for all mass fractions between "100% dispatchable" and "100% energy storage" at a duty cycle of 8 h-16 h. This CPG-F facility costs \$173 M. This system cost is 50% higher than that of an energy-maximized CPG power plant and only 3% higher than the cost of the most expensive CPG-F facility designed to provide only energy storage over an 8h-16h duty cycle. This increase in cost is mainly due to the slightly larger flow rates that the system can achieve. Thus, the costs of a CPG-F facility, designed to provide anywhere between 100% dispatchable power and 100% energy storage, are close to the costs for a CPG-F facility designed to only provide energy storage, but with the former providing significantly more flexibility to react to price signals from the electricity market.

4. Conclusions and suggestions for future investigations

This paper has demonstrated how a CO₂ Plume Geothermal (CPG) power plant can be expanded to a Flexible-CPG (CPG-F) facility by adding wells and a second, shallow reservoir. Unlike a CPG power plant, CPG-F facilities may be designed to provide dispatchable power, energy storage over a range of charge and discharge cycle durations (i.e., duty cycles), or both dispatchable power and energy storage *simultaneously*—providing baseload power with dispatchable storage for demand response. While this flexibility, coupled with the additional incentive for geologically storing CO₂, likely means that CPG-F facilities will be valuable to decarbonization efforts broadly, designing any given CPG-F facility is non-trivial. For example, there are multiple optimum design points (e.g., minimum cost, maximum power, maximum net

energy) that may be in tension or have non-intuitive relationships with one another. As a result, in this study, an initial investigation into these relationships and design criteria was conducted. Some of the primary findings include:

- 1. A CPG-F facility can deliver more instantaneous power than a CPG power plant, but at the expense of decreased net energy production because a CPG-F facility, operated for energy storage, has a lower efficiency than a CPG power plant (Fig. 4).
- 2. The CO₂ circulation rate that maximizes net power production is different than the rate that minimizes the specific capital cost when a CPG-F facility is designed to provide dispatchable power (Fig. 3). But these flowrates are generally the same or close to the same when the facility is designed to provide energy storage (Fig. 5).
- 3. While the duty cycle of a CPG-F facility, designed to provide energy storage, is an operational decision, duty cycle decisions may influence the ability to operate at optimal design points. For example, a CPG-F facility, designed for energy storage, produces power more efficiently over duty cycles of equal durations (e.g., 12h-12h), compared to duty cycles of unequal durations (e.g., 4h-20h) (Fig. 4). Further, the maximum power produced by a CPG-F facility, designed to provide energy storage, may be impossible to reach because the temperature of the produced fluid can decrease below ambient air temperatures (Fig. 5).
- 4. The power capacity and capital cost of a CPG-F facility, designed to provide only energy storage, increases with shorter duty cycle durations, but can provide a similar amount of energy across all duty cycles as a CPG-F facility, designed to only provide dispatchable power (Fig. 4).
- 5. Across all cases considered, the total project capital cost of a CPG-F facility, designed for a given energy storage duty cycle, is 34% to 65% greater than the cost of a CPG power plant; the total project capital cost of a CPG-F facility, designed to provide energy storage over all durations, is 70% greater than that of a CPG power plant (Fig. 7). This increase in cost is largely due to the increased drilling and well completion costs and the increased size of the surface equipment. However, due to the increased production power of the CPG-F facility, the specific capital cost of a CPG-F facility decreases below that of a CPG power plant.
- 6. Compared to a CPG-F facility, designed to provide only energy storage, designing a CPG-F facility to provide dispatchable power and energy storage simultaneously generally results in an increased daily net energy production and a decreased daily power output. However, there are some scenarios, where it is possible to produce more daily net energy and power output (Fig. 9). Also, a CPG-F facility, designed to provide dispatchable power and energy storage simultaneously, only costs 3% more than a CPG-F facility designed to provide only energy storage (Fig. 9).

Future decarbonized electricity systems will likely be comprised of a portfolio of technologies and processes that work synergistically to meet demand. The results show that the CPG-F facility has promise in these future decarbonized electricity systems because they demonstrate that a single electricity system component can provide many different services: geologic $\rm CO_2$ storage, dispatchable power, energy storage, and both dispatchable power and energy storage simultaneously. Here, a few directions for potential future work, that was outside the scope of this initial CPG-F investigation, but build off its findings, are provided:

• Pursue design modifications that increase the power production capacity (and power storage capacity, if applicable) of a CPG-F facility. In this study, one horizontal injection well and one horizontal production well in each aquifer were assumed, but a CPG-F facility could be scaled by increasing the number of wells because more wells would enable larger injection and production flowrates. But adding and using more wells would 1) increase the cost of a CPG-F facility and 2)

increase the rate that the geothermal heat resource is depleted. As a result, future work could also investigate the cost and heat-depletion tradeoffs that are introduced when this design modification is considered, similar to the work by [30] for CPG systems.

- Investigate energy storage duty cycles that are longer than 24 hours. It is likely that technologies that can provide long duration energy storage (e.g., weeks or months of storage) will have value in future low-carbon electricity systems and it is possible for a CPG-F facility to operate over durations greater than single days [48,56,57]. In this study, the duty cycle was limited to 24-hour periods, but the deep aquifers that are targets for geologic CO₂ storage may enable long-duration energy storage because they have the capacity to store large volumes of fluids. For example, these subsurface formations underlie half of North America [58,59]. As a result, if electricity market rules are created to incentivize long-duration energy storage, technologies like CPG-F may be uniquely positioned to provide these services.
- Conduct a parametric analysis that covers a wide range of reservoir, well, and surface power plant parameters to evaluate the CPG-F system performance and what operational parameters should consequently be chosen. In the current study we limited the operation to a single reservoir and surface parameter set, however, it is likely that CPG-F facilities can be operated economically under a wide range of reservoir and ambient conditions. Thus, a future sensitivity study of CPG-F systems should investigate parameters such as reservoir permeability, permeability anisotropy, porosity, thickness, and depth as well as various ambient air heat rejection temperatures and geothermal temperature gradients to identify suitable system operation conditions.
- Integrate a CPG-F facility into an energy system model to investigate how it is optimally dispatched and quantify its value. Prior work integrated CO₂-BES facilities into optimization-based, systems-level, models [40,41]. A similar approach could be taken for CPG-F facilities [40,41]. Given the increased flexibility of a CPG-F facility, compared to a CO₂-BES facility, this avenue for future work would likely be particularly helpful in guiding future CPG-F system design modifications (e.g., those that investigate scaling-up a CPG-F facility). For example, if integration with a system model demonstrated that it was most profitable to provide both energy storage and dispatchable power simultaneously, future work could focus specifically on optimizing the CPG-F design for that service. Additionally, it is recommended that a risk analysis of CPG-F systems be conducted in the future to aid potential system operators in implementing and operating the CPG-F technology. Further, future integration studies could also consider how decarbonization policies (i.e., a CO2 price) could influence how a CPG-F facility should be operated to maximize profit. In the design considered for this study, over 15 MtCO2 were injected during the development of the deep reservoir and the maximum project capital cost was just under \$200 million. As a result, if CPG-F operators were compensated for storing CO₂ at a rate of \$14/tCO₂, the revenue from storing CO₂ would exceed the capital cost of the most expensive CPG-F facility investigated in this study. For reference, both the social cost of carbon and 45Q tax incentive in the US. are larger than \$14/tCO₂ [60,61]. As a result, depending on the electricity prices and the rate at which operators are compensated for storing CO₂, the value of providing CO₂ storage services may influence design and operation decisions more than the value of providing grid services.

CRediT authorship contribution statement

Mark R. Fleming: Conceptualization, Methodology, Software, Validation, Formal analysis, Investigation, Data curation, Writing – original draft, Visualization. **Benjamin M. Adams:** Conceptualization, Methodology, Formal analysis, Investigation, Supervision, Writing –

original draft, Visualization. **Jonathan D. Ogland-Hand:** Writing – original draft. **Jeffrey M. Bielicki:** Writing – review & editing. **Thomas H. Kuehn:** Supervision, Writing – review & editing. **Martin O. Saar:** Funding acquisition, Resources, Writing – review & editing.

Declaration of Competing Interest

The authors declare that they have no known competing financial interests or personal relationships that could have appeared to influence the work reported in this paper.

Acknowledgments

We gratefully acknowledge funding from the National Science Foundation (NSF) under the Sustainable Energy Pathways (SEP) Grant SEP-123069, the NSF National Research Traineeship (Grant 1922666) and the Sloan Foundation, and the Innovations at the Nexus of Food, Energy, and Water Systems (INFEWS) Grant 1739909; and the Sustainability Institute and the Center for Energy Research, Training, and Innovation (CERTAIN) at the Ohio State University (OSU). We also thank the Initiative for Renewable Energy and the Environment (IREE), a signature program of the Institute on the Environment (IonE) at UMN for initial CPG research support. We furthermore thank the Werner Siemens Foundation (Werner Siemens-Stiftung) for their support of the Geothermal Energy and Geofluids (GEG.ethz.ch) Group at ETH Zurich, Switzerland. Any opinions, findings, conclusions, or recommendations in this material are those of the authors and do not necessarily reflect the views of the NSF, UMN, OSU, IREE, IonE, the Werner Siemens Foundation, the GEG Group or ETH Zurich. We also thank the anonymous reviewers for their helpful comments and suggestions that improved an earlier version of the manuscript.

Appendix A. Supplementary data

Supplementary data to this article can be found online at https://doi.org/10.1016/j.enconman.2021.115082.

References

- Krey V, Luderer G, Clarke L, Kriegler E. Getting from here to there energy technology transformation pathways in the EMF27 scenarios. Clim Change 2014; 123(3-4):369–82. https://doi.org/10.1007/s10584-013-0947-5.
- [2] Kriegler E, Weyant JP, Blanford GJ, Krey V, Clarke L, Edmonds J, et al. The role of technology for achieving climate policy objectives: overview of the EMF 27 study on global technology and climate policy strategies. Clim Change 2014;123(3-4): 353-67. https://doi.org/10.1007/s10584-013-0953-7.
- [3] Audoly R, Vogt-Schilb A, Guivarch C, Pfeiffer A. Pathways toward zero-carbon electricity required for climate stabilization. Appl Energy 2018;225:884–901. https://doi.org/10.1016/j.apenergy.2018.05.026.
- [4] IPCC. Global warming of 1.5°C: An IPCC Special Report on the impacts of global warming of 1.5°C above pre-industrial levels and related global greenhouse gas emission pathways, in the context of strengthening the global response to the threat of climate change, sustainable development, and efforts to eradicate poverty. 2018.
- [5] Gambhir A, Rogelj J, Luderer G, Few S, Napp T. Energy system changes in 1.5 °C, well below 2 °C and 2 °C scenarios. Energy Strategy Reviews 2019;23:69–80. https://doi.org/10.1016/j.esr.2018.12.006.
- [6] Sepulveda NA, Jenkins JD, de Sisternes FJ, Lester RK. The Role of Firm Low-Carbon Electricity Resources in Deep Decarbonization of Power Generation. Joule 2018;2 (11):2403–20. https://doi.org/10.1016/j.joule.2018.08.006.
- [7] Jayadev G, Leibowicz BD, Kutanoglu E. U.S. electricity infrastructure of the future: Generation and transmission pathways through 2050. Applied Energy 2020;260: 114267. doi:10.1016/j.apenergy.2019.114267.
- [8] Bistline JET, Blanford GJ. Value of technology in the U.S. electric power sector: Impacts of full portfolios and technological change on the costs of meeting decarbonization goals. Energy Economics 2020;86:104694. https://doi.org/ 10.1016/j.eneco.2020.104694.
- [9] Brown DW. A Hot Dry Rock Geothermal Energy Concept Utilizing Supercritical CO2 Instead of Water. In: Proceedings of the Twenty-Fifth Workshop on Geothermal Reservoir Engineering; 2000. p. 1-6.
- [10] Atrens AD, Gurgenci H, Rudolph V. CO2 Thermosiphon for Competitive Geothermal Power Generation. Energy Fuels 2009;23(1):553–7. https://doi.org/ 10.1021/ef800601z.

- [11] Atrens AD, Gurgenci H, Rudolph V. Electricity generation using a carbon-dioxide thermosiphon. Geothermics 2010;39(2):161–9. https://doi.org/10.1016/j. geothermics.2010.03.001.
- [12] Adams BM, Kuehn TH, Bielicki JM, Randolph JB, Saar MO. A comparison of electric power output of CO2 Plume Geothermal (CPG) and brine geothermal systems for varying reservoir conditions. Appl Energy 2015;140:365–77. https:// doi.org/10.1016/j.apenergy.2014.11.043.
- [13] Randolph JB, Adams BM, Kuehn TH, Saar MO. Wellbore Heat Transfer in CO2based Geothermal Systems. Geothermal Resources Council Transactions 2012;36.
- [14] Pruess K. Enhanced geothermal systems (EGS) using CO2 as working fluid—A novel approach for generating renewable energy with simultaneous sequestration of carbon. Geothermics 2006;35(4):351–67. https://doi.org/10.1016/j.geothermics.2006.08.002
- [15] Pruess K. On production behavior of enhanced geothermal systems with CO2 as working fluid. Energy Convers Manage 2008;49(6):1446–54. https://doi.org/ 10.1016/j.enconman.2007.12.029.
- [16] Pruess K. Enhanced geothermal systems (EGS): comparing water and CO2 as heat transmission fluids. Proceedings of the New Zealand geothermal workshop, Auckland, New Zealand: 2007, p. 1–13.
- [17] Randolph JB, Saar MO. Combining geothermal energy capture with geologic carbon dioxide sequestration. Geophysical Research Letters 2011:38. https://doi. org/10.1029/2011GL047265.
- [18] Randolph JB, Saar MO. Impact of reservoir permeability on the choice of subsurface geothermal heat exchange fluid: CO2 versus water and native brine. Geothermal Resources Council Transactions 2011;35.
- [19] IPCC. IPCC Special Report on Carbon Dioxide Capture and Storage. Cambridge, United Kingdom: Cambridge University Press; 2005.
- [20] Bielicki JM, Pollak MF, Fitts JP, Peters CA, Wilson EJ. Causes and financial consequences of geologic CO2 storage reservoir leakage and interference with other subsurface resources. Int J Greenhouse Gas Control 2014;20:272–84. https:// doi.org/10.1016/J.IJGGC.2013.10.024.
- [21] Bielicki JM, Peters CA, Fitts JP, Wilson EJ. An examination of geologic carbon sequestration policies in the context of leakage potential. Int J Greenhouse Gas Control 2015;37:61–75. https://doi.org/10.1016/j.ijggc.2015.02.023.
- [22] Bielicki JM, Pollak MF, Deng H, Wilson EJ, Fitts JF, Peters CA. The Leakage Risk Monetization Model for Geologic CO2 Storage. Environ Sci Technol 2016;50(10): 4923–31. https://doi.org/10.1021/acs.est.5b0532910.1021/acs.est.5b05329. 6001
- [23] Gibbins J, Chalmers H. Carbon capture and storage. Energy Policy 2008;36(12): 4317–22. https://doi.org/10.1016/j.enpol.2008.09.058.
 [24] Garapati N, Randolph JB, Saar MO. Brine displacement by CO2, energy extraction
- [24] Garapati N, Randolph JB, Saar MO. Brine displacement by CO2, energy extraction rates, and lifespan of a CO2-limited CO2-Plume Geothermal (CPG) system with a horizontal production well. Geothermics 2015;55:182–94. https://doi.org/ 10.1016/i.geothermics.2015.02.005.
- [25] Randolph JB, Saar MO. Coupling carbon dioxide sequestration with geothermal energy capture in naturally permeable, porous geologic formations: Implications for CO2 sequestration. Energy Procedia 2011;4:2206–13. https://doi.org/ 10.1016/j.egypro.2011.02.108.
- [26] Garapati N, Randolph JB, Valencia JL, Saar MO. CO2-Plume Geothermal (CPG) Heat Extraction in Multi-layered Geologic Reservoirs. Energy Procedia 2014;63: 7631–43. https://doi.org/10.1016/j.egypro.2014.11.797.
- [27] Fleming MR, Adams BM, Kuehn TH, Bielicki JM, Saar MO. Increased Power Generation due to Exothermic Water Exsolution in CO2 Plume Geothermal (CPG) Power Plants. Geothermics 2020;88:101865. https://doi.org/10.1016/j. geothermics 2020 101865
- [28] Ezekiel J, Adams BM, Saar MO, Ebigbo A. Numerical analysis and optimization of the performance of CO2-plume geothermal (CPG) production wells and implications for electric power generation (under review). Geothermics 2022;98: 102270. https://doi.org/10.1016/j.geothermics.2021.102270.
- [29] Adams BM, Kuehn TH, Bielicki JM, Randolph JB, Saar MO. On the importance of the thermosiphon effect in CPG (CO2 plume geothermal) power systems. Energy 2014;69:409–18. https://doi.org/10.1016/j.energy.2014.03.032.
- [30] Adams BM, Vogler D, Kuehn TH, Bielicki JM, Garapati N, Saar MO. Heat depletion in sedimentary basins and its effect on the design and electric power output of CO2 Plume Geothermal (CPG) systems. Renewable Energy 2021;172:1393–403. https://doi.org/10.1016/j.renene.2020.11.145.
- [31] Randolph JB, Saar MO, Bielicki JM. Geothermal Energy Production at Geologic CO2 Sequestration sites: Impact of Thermal Drawdown on Reservoir Pressure. Energy Procedia 2013;37:6625–35. https://doi.org/10.1016/j. egypro.2013.06.595.
- [33] Ezekiel J, Ebigbo A, Adams BM, Saar MO. Combining natural gas recovery and CO2-based geothermal energy extraction for electric power generation. Appl Energy 2020;269:115012. https://doi.org/10.1016/j.apenergy.2020.115012.
- [34] Hefny M, Qin CZ, Saar MO, Ebigbo A. Synchrotron-based pore-network modeling of two-phase flow in Nubian Sandstone and implications for capillary trapping of carbon dioxide. International Journal of Greenhouse Gas Control 2020:103. https://doi.org/10.1016/j.ijggc.2020.103164.

- [35] Saar MO, Randolph JB, Kuehn TH. Carbon Dioxide-Based Geothermal Energy Generation Systems and Methods Related Thereto. US Patent 2012;8316955:B2.
- [36] Adams BM. On the Power Performance and Integration of Carbon-dioxide Plume Geothermal (CPG) Electrical Energy Production (Doctoral dissertation). University of Minnesota; 2015. p. 1–168.
- [37] Buscheck TA, White JA, Carroll SA, Bielicki JM, Aines RD. Managing geologic CO2 storage with pre-injection brine production: a strategy evaluated with a model of CO2 injection at Snøhvit. Energy Environ Sci 2016;9(4):1504–12. https://doi.org/ 10.1039/C5EE03648H.
- [38] Liu H, He Q, Borgia A, Pan L, Oldenburg CM. Thermodynamic analysis of a compressed carbon dioxide energy storage system using two saline aquifers at different depths as storage reservoirs. Energy Convers Manage 2016;127:149–59. https://doi.org/10.1016/j.enconman.2016.08.096.
- [39] Garapati N, Adams BM, Fleming MR, Kuehn TH, Saar MO. Combining brine or CO2 geothermal preheating with low-temperature waste heat: A higher-efficiency hybrid geothermal power system. Journal of CO2 Utilization 2020;42:101323. https://doi.org/10.1016/j.jcou.2020.101323.
- [40] Ogland-Hand JD, Bielicki JM, Adams BM, Nelson ES, Buscheck TA, Saar MO, et al. The value of CO2-Bulk energy storage with wind in transmission-constrained electric power systems. Energy Convers Manage 2021;228:113548. https://doi. org/10.1016/j.enconman.2020.113548.
- [41] Ogland-Hand JD, Bielicki JM, Wang Y, Adams BM, Buscheck TA, Saar MO. The value of bulk energy storage for reducing CO2 emissions and water requirements from regional electricity systems. Energy Convers Manage 2019;181:674–85. https://doi.org/10.1016/j.enconman.2018.12.019.
- [42] Buscheck TA, Bielicki JM, Edmunds TA, Hao Y, Sun Y, Randolph JB, et al. Multifluid geo-energy systems: Using geologic CO2 storage for geothermal energy production and grid-scale energy storage in sedimentary basins. Geosphere 2016; 12(3):678–96. https://doi.org/10.1130/GES01207.1.
- [43] Buscheck TA, Bielicki JM, Chen M, Sun Y, Hao Y, Edmunds TA, et al. Integrating CO2 Storage with Geothermal Resources for Dispatchable Renewable Electricity. Energy Procedia 2014;63:7619–30. https://doi.org/10.1016/j. egypty.2014.17.766
- [44] Adams BM, Kuehn TH, Randolph JB, Saar MO. The Reduced Pumping Power Requirements from Increasing the Injection Well Fluid Density. GRC Transactions 2013;37:667–72.
- [45] Pruess K, Oldenburg CM, Moridis G. TOUGH2 User's Guide, Version 2. Report LBNL-43134, Lawrence Berkeley National Laboratory, California 1999.
- [46] Pruess K. ECO2N: A TOUGH2 Fluid Property Module for Mixtures of Water, NaCl, and CO2. Report LBNL-57952 Lawrence Berkeley National Laboratory, California 2005
- [47] Klein SA, Alvarado F. Engineering Equation Solver. F-Chart Software 2002.
- [48] Fleming M.R., Adams B.M., Randolph J.B., Ogland-Hand J.D., Kuehn T.H., Buscheck T.A., et al. High Efficiency and Large-scale Subsurface Energy Storage with CO2. 43rd Workshop on Geothermal Reservoir Engineering Stanford, CA, Palo Alto. California: 2018.
- [49] Fleming M. The Performance of a Carbon-Dioxide Plume Geothermal Energy Storage System (Doctoral Dissertation), University of Minnesota; 2019, p. 1–255.
- [50] Garapati N, Adams BM, Bielicki JM, Schaedle P, Randolph JB, Kuehn TH, et al. A Hybrid Geothermal Energy Conversion Technology - A Potential Solution for Production of Electricity from Shallow Geothermal Resources. Energy Procedia 2017;114:7107–17. https://doi.org/10.1016/j.egypro.2017.03.1852.
- [51] Welch P, Boyle P. New turbines to Enable Efficient Geothermal Power Plants. Geotherm Resour Counc Trans 2009;33:8.
- [52] Span R, Wagner W. A new equation of state for carbon dioxide covering the fluid region from the triple-point temperature to 1100 K at Pressures up to 800 MPa. J Phys Chem Ref Data 1996;25(6):1509–96. https://doi.org/10.1063/1.555991.
- [53] Farshad FF, Garber JD, Rieke HH, Komaravelly SG. Predicting corrosion in pipelines, oil wells and gas wells; a computer modeling approach. Sci Iran Trans C: Chem Chem Eng 2010;17:86–96.
- [54] Moody LF. Friction factor for pipe flow. Trans ASME 1944;66:671-84.
- [55] Adams B.M., Ogland-Hand J.D., Bielicki J.M., Schaedle P., Saar M.O. Estimating the Geothermal Electricity Generation Potential of Sedimentary Basins Using genGEO (The Generalizable GEOthermal Techno-Economic Simulator). doi: 10.26434/chemrxiv.13514440.v1.
- [56] Dowling JA, Rinaldi KZ, Ruggles TH, Davis SJ, Yuan M, Tong F, et al. Role of Long-Duration Energy Storage in Variable Renewable Electricity Systems. Joule 2020;4 (9):1907–28. https://doi.org/10.1016/j.joule.2020.07.007.
- [57] Guerra OJ, Zhang J, Eichman J, Denholm P, Kurtz J, Hodge B-M. The value of seasonal energy storage technologies for the integration of wind and solar power. Energy Environ Sci 2020;13(7):1909–22. https://doi.org/10.1039/D0EE00771D.
- [58] National Energy Technology Laboratory. Carbon Storage Atlas: Fifth Edition. 2015.
- [59] Coleman JL, Cahan SM. Preliminary catalog of the sedimentary basins of. the United States; 2012.
- [60] 26 United States Code Section 45Q (2021): Credit for carbon oxide sequestration. https://uscode.house.gov/view.xhtml?req=(title:26section:45Qedition:prelim).
- [61] Environmental Protection Agency (EPA). The Social Cost of Carbon. https:// 19january2017snapshot.epa.gov/climatechange/social-cost-carbon_html.